Gel Dosimetry

THE DEVELOPMENT OF A LOW DENSITY RADIOCHROMIC GEL DOSIMETER

by

HAILAH AL RASHED, B.Phys

A Thesis

Submitted to the School of Graduate Studies

in Partial Fulfillment of the Requirements

for the Degree

Master of Science

McMaster University

Master of Science (2018) McMaster University

(Medical Physics) Hamilton, ON

TITLE: The Development of a Low Density Radiochromic Gel Dosimeter.

AUTHOR: HAILAH AL RASHED, B.Phys.

SUPERVISOR: Dr. Kevin Diamond

NUMBER OF PAGES: xii, 90

Abstract

This research aims to develop a tissue-mimicking material and produce a 3D gelatin that has density of approximately a human lung, which is in the ranges of (0.25 – 0.35) g/cm^3. Tissue equivalent models are important in order to study the radiation dose planned for patients. To achieve the desired density of a human tissue, different types of gelatin were whisked for 300 seconds using a typical hand mixer. The mechanical properties of the gelatin mixtures, standard and foamed, were evaluated by applying different forces.

The mechanical properties for the gels were measured using an indentation technique, which showed that the gels act as elastic materials. The mechanical properties of the foams were also evaluated. Mixtures that contained 300 bloom gelatin, glycerol, and sorbitol, were whisked for 60, 180, 300 seconds to achieve different densities evaluated by CT imaging. The density of the180 - and 300 - seconds gelatin foams were found to be 0.33 ± 0.16 and 0.33 ± 0.052 g/cm^3, respectively, which is similar to the human lung density. Finally, FXO gel sheets and the FXO foam sheets were irradiated and the radiosensitivity quantified by measuring transmission using a spectrometer. The change in the attenuation coefficient was linear with dose.

Keywords:

Gel Dosimetry, Radiation Dosimetry, Radiochromic Dosimeter, Radiotherapy, Quality Assurance (QA), Gelatin, Two dimensional, Three dimensional

Table of Contents

Abstract……..……iv

Acknowledgment……...……..ix

List of Figures ……..……..…….…....x

List of Tables……...……xii

1. Introduction ***1***

1.1 Quality assurance in radiation therapy **2**

1.2 Gel dosimetry **4**

1.2.1 History 4

1.2.2 Fricke Gel Dosimeters 5

1.2.3 Polymer Gel Dosimeters 8

1.2.4 Radiochromic Gel Dosimeters 10

1.2.5 F(B)X-type Radiochromic Dosimeters 11

1.3 Tissue-Mimicking Phantoms **11**

1.3.1 Definition of tissue mimicking material (TMM) 13

1.3.2 Manufacturing 14

1.3.3 Application of Gelatin as Tissue-Mimicking Material 16

1.3.4 Simulation of Lungs 17

1.4 Gelatin **19**

1.4.1 History 19

1.4.2 Elastic Properties 26

1.4.3 Low Density Foams 27

1.5 Measurement of Elastic Properties 28

1.5.1 Indentation 29

1.5.2 Needle Penetration 30

1.6 Optical Transmission Measurements 32

1.6.1 Optical Properties 33

1.6.2 Optical Transmission 35

1.6.3 Effect of Scattering on Light Transmission Through a Slab 36

1.7 Thesis Proposal 37

2. Methods and Materials 38

2.1 Gelatin Fabrication 38

2.1.1 Gelatin Indentation 39

2.2 Gelatin Foam Fabrication 40

2.2.1 Gelatin Foam Indentation 41

2.2.2 Gelatin Foam CT Scan 42

2.3 Ferrous-Xylenol Orange (FXO) Gel Fabrication 43

3. Elastic and Radiological Properties of Gelatin 48

4. Dose Response 60

5. Discussion 64

6. Conclusion 66

7. Future Work 67

8. References 68

Acknowledgment

I would like to express my deepest appreciation to everyone who helped in this research. I extend my sincere gratitude to Dr. Kevin Diamond, my supervisor, for his support, guidance and encouragement. I am privileged that he shared his exceptional knowledge to help in the fulfillment of my thesis.

To Dr.Tom Ferral and Dr.MarcinWierzbicki for their valuable comments and help.

Also, I thank Weaam, Meshariy, Monerra, Abdulrahman and Fearas for their support and encouragement throughout this journey.

To my loved ones Nawwaf, Mayar and Saud I hope my journey will inspire you to achieve your goals no matter how hard it gets.

To Abdullah thanks for all the support through this journey.

To my mother, Madawey my words cannot express the gratitude to your endless support and encouragement, everything I achieved until now is because of you.

To my father, Abdulmohsen wish you were here, always loved and missed.

List of Figures

Figure 1-1: The development of radiotherapy over the years [2]. 3

Figure 1-2 The gross anatomy of the human lungs [70]. 17

Figure 1-3 : The gelatin production process from the GMIA handbook [22]..... 21

Figure 1-4 : The effect of time on the gelatin strength of a 6 2/3% gel at 10 ℃ [22].. 23

Figure 1-5 : The effect of bloom on the gel concentration at 10 ℃ [22] 24

Figure 1-6 : The effect of gelatin concentration at 60 ℃ on the viscosity which has a unit of centipoise (cps) [22]. 25

Figure 1-7: Electromagnetic wave spectrum [33]. 34

Figure 1-8 The course of light transmission through a material [33]. 35

Figure 2-1: The apparatus used in finding the mechanical properties of gels and foamed gels. 40

Figure 2-2: The left picture is the FXO gelatin thin sheet, as for the right one it is the foamed FXO gelatin. 44

Figure 2-3: The left picture is for the gel FXO after irradiation, as the picture on the right is for the foamed gel FXO after irradiation. 46

Figure 2-4 A sketch of the linear spectroscopy apparatus. Where (a) is the fiber optic lluminator device, (b) is the plastic holder that holds the gelatin sheet with a window in the middle, (c) is the Ocean Optics spectrometer (HR4000), (d) the computer that hold the Ocean View analysis system. 47

Figure 3-1 The effect of force on different concentrations of 220 bloom gelatin cubes in a line graph..... 49

Figure 3-2 the effect of force on different concentrations of 300 bloom gelatin in a line graph..... 50

Figure 3-3 The effect of major force (g) on the (a)15% 220 bloom gelatin+ sorbitol foam and (b 15% 300 bloom gelatin+ sorbitol foam cubes. 52

Figure 3-4 The effect of major force (g) on the (a)15% 220 bloom gelatin+ glycerol foam and (b)15%300 bloom gelatin+glycerol foam cubes. 53

Figure 3-5 The effect of major force (g) on the (a)15% 220 bloom gelatin+ sorbitol and glycerol mixture foam and (b)15%300 bloom gelatin+ sorbitol and glycerol mixture foam cubes. Sorgly= sorbitol+glycerol. 54

Figure 3-6 The stress and strain curve for (a) 15% 220 bloom+ sorbitol and glycerol mixture and (b) 15% 300 bloom + sorbitol and glycerol. 57

Figure 3-7 The stress and strain curve of (a) 200 bloom gelatin with different concentrations and (b) 300 bloom gelatin of different concentrations. 58

Figure 4-1 The effects of radiation on thin gelatin FXO sheets in blue, FXO gelatin sheets foamed for 2min in gray and FXO gelatin sheets for 5min in orange. 61

Figure 4-2 The relation between the irradiation dose and the mass attenuation coefficient..... 62

List of Tables

Table 1-1 Fricke gel dosimeter ion diffusion measurements as observed in Baldock et al [35].Were : A = agar, agarose = agar, G = gelatin, PVA = polyvinyl alcohol, S = sulfuric acid H2 SO4 , XO = xylenol orange, BE = benzoic acid , Fo = formaldehyde, P = phenanthrol 6

Table 1-2 A summary of the chemicals used to fabricate tissue mimicking materials. TMM:Tissue mimicking material, SC: Silicon chloride, Pc: Potassium chloride [65]. 16

Table 1-3 The amino acid obtained after the hydrolysis of the gelatin [22]. 22

Table 2-1 Gelatin preparation in different concentrations. 39

Table 2-2 The different concentration of sorbitol and glycerol added to the gelatin... 41

Table 2-3 The FXO gels preparation method. 44

1. Introduction

In order to achieve the accurate evaluation of radiation dose for patients, a need arises for the production of a material that imitates human tissue. These phantoms maybe used in many experiments to observe the reaction of the human skin/system when applying different doses to it. This procedure is important to be performed before delivering the treatment to patients to ensure that the intended dose is delivered accurately.

This research aims to produce a tissue equivalent material and manufacture a 3D gelatin that has the density of a human lung, which is in the ranges of (0.25 – 0.35) g/cm^3. The gelatin was whisked for up to 300 seconds using a typical hand mixer to achieve the desired density. The mechanical properties of the gelatin mixture and the foam gelatin were evaluated by applying different forces and is discussed in detail in sections 2.1.1 and 2.2.1, respectively.

The gelatin dose response was visible as it changed its colour after being irradiated using a linear accelerator. The colour transformation was due to (Fe^{2+}) being converted to (Fe^{3+}) upon irradiation. Colour changes were evaluated using optical spectroscopy and compared to the delivered doses, explained in detail in chapter 3. A treatment planning system, Pinnacle, was used to analyze the composition of the cubes of gelatin and foam.

1.1 Quality assurance in radiation therapy

The goal of quality assurance (QA) is to ensure effective patient treatments and evaluating the system used in the radiation therapy to achieve the optimal quality. Ideally, the treatment plan for each patient would have minimal effect on normal tissue or none at all. It is well known that when using radiation, the radiation oncologist should verify that the correct dose is delivered to the cancer cells and to avoid impacting the normal tissues. Thus, assuring the correctness of this procedure before providing the treatment to the patient, a tissue-mimicking material such as gelatin phantoms may be used to verify that the dose distribution is accurate. The use of radiation therapy is not limited to destroying a tumour; it is also used as a palliative treatment to control the pain for these patients and help them feel more comfortable by shrinking local disease. The benefits of quality assurance in radiation therapy are but not limited to: reducing errors in treatment delivery, verifying performance of radiation equipment, and more dependable comparisons of results between cancer centers.

From Prabhakar (2013) [1], intensity modulated radiation therapy (IMRT) and /or volumetric modulated arc therapy (VMAT) is used to perform a patient specific quality assurance (QA) that aims to deliver a correct dose to the tumour.

In, Bernier *et al*. [2] and Owen *et al*. [3] the different machine types, such as Magnetic resonance imaging (MRI), computed tomography

(CT), volumetric arc therapy (VMAT), cone beam computed tomography (CBCT) and many others were developed from the 1970's until now. The technology in radiation therapy has developed rapidly since the discovery of the x-ray in 1895 as seen in (Figure 1-1). Many different techniques have been developed since then and helped in the revolution of radiation therapy. The best know irradiation techniques in radiation therapy are: IMRT, Tomotherapy, VMAT, SRS and the Cyberknife. There are factors that need to be considered when treating the patient to ensure minimal errors such as the patient alignment or setup, which if was not correctly performed can lead to misdosing of the patient.

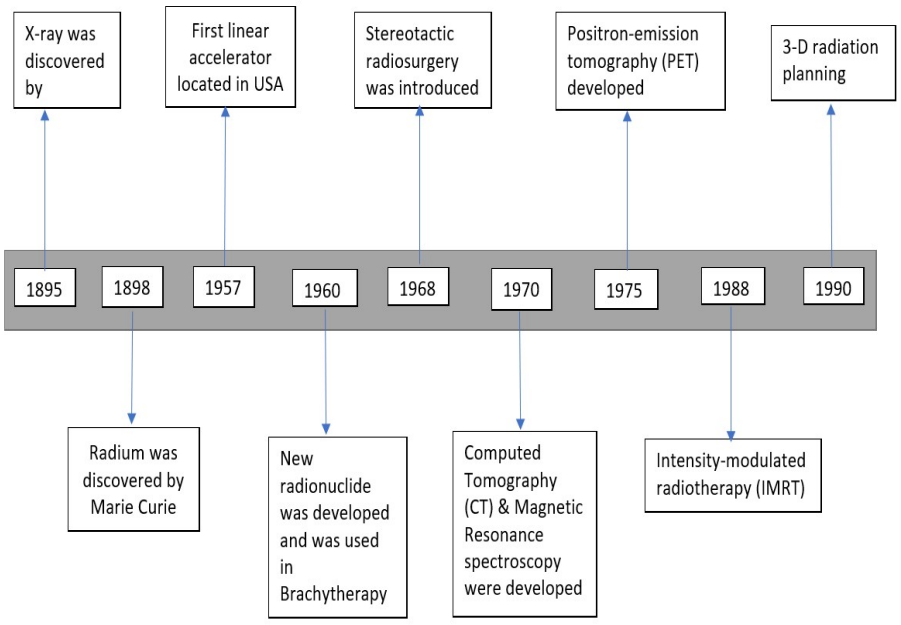

Figure 1-1: The development of radiotherapy over the years [2].

1.2 Gel dosimetry

The gel dosimetry is a very important tool in the radiation therapy field. It contributes in establishing a solid base for treating cancer. Also, it is a useful tool in performing the quality assurance to minimize and/or prevent any errors in these treatments. Hence, when using gel dosimeters, it helps in enhancing the precision and accuracy of the treatment because the medical physicist can reproduce the treatment circumstances using these tissue equivalent materials [5,6,7,8].

1.2.1 History

Gel dosimeters were first demonstrated in 1950 by Day and Stein [9], where they used agar and gelatin as gelling agents. They added some dyes such as: methylene blue, pheno-indo-2 : 6-di-chlorophenol, and Folin's phenol reagent to them that changed colour upon radiation, where they found that the change in the dye colour was due mostly to the absorbed dose, although there is a small reaction because of electron capture that helps in the actions of the ionizing radiation.

In 1957 Andrew, Murphy *et al.* [10] found that the use of agar gels in a specific concentration made the gel stay intact after it was removed from the mould. They added chloral hydrate to the gel mixture that, when irradiated, changed to HCl. Thus, the mixture's conductivity and pH were altered and quantified using spectrophotometry and pH analyses. In addition, they were able to observe the radiation depth dose using the spectrometer [10,28].

The most well known work about gel dosimeter was the publication of Gore *et al*. in 1984. They investigated the Fricke dosimeter used with a gelling agent and Xylenol orange (XO) chelator, which changes its colour when bound Fe^{+2} is converted to Fe^{+3} [28,11].

Polymer gel dosimeters were developed later, observed in Alexander *et al.* [12]. Monomers contained in these dosimeters polymerized due to irradiation [12,28]

From Low (2015) [25], as radiation dosimetry has evolved in the last century there has arisen a need for 3-D dosimetry approaches due to the complexity of the delivered dose distributions.

1.2.2 Fricke Gel Dosimeters

Most of the gel dosimeters developed from the Fricke gel which is the best approach to measure the absorbed dose in 3D, due to the easy fabrication. In 1984 Gore *et al*. [11] investigated phantoms fabricated from Fricke gel with the addition of Xylenol orange (XO) that, when irradiated, changed its colour. When Fricke gels are irradiated, the ferrous (Fe^{2+}) changes to ferric (Fe^{3+}). The change was evaluated using magnetic resonance imaging (MRI) that measured the (R1 & R2), which are known as the spin-lattice and spin-spin relaxation rates respectively. However, the Fricke gel has an issue of diffusion after the irradiation, which affects the accumulated dose distribution [11]. Also, the MRI is not accessible all the time due to its increased use for clinical applications. It was observed by Appleby *et al.* [34] that the

distribution of the Fricke mixture in the gelling agent could lead to 3D gel dosimeters that could be read by MRI. However, it was also noted that these Fricke gel dosimeters experienced significant ion diffusion after they were irradiated, causing the unstable dose distributions [28]. Development of this type of gel dosimeter was limited until ion diffusion could be addressed, which was discussed in 2001 by Baldock (table 1-1) [35,28].

Reference	Diffusion Coefficient (10^{-3} cm^2h^{-1})	Gel Type & Concentration (%)	Other Constituents (mM)	Temperature (°C)
Schulz (1990)	18.3±1.4	A 1	S 12.5, Fe3+ 1	-
Schulz (1990)	15.8±1.1	A 1	S 25, Fe3+ 1	-
Olsson (1992)	19.1±1.0	A 1.5	S 50, Fe2+ 1	25
Gambarini (1994)	10.9±1.6*	A 1	S 50, Fe2+ 1, NaCl 1	15-17.5
Balcom (1995)	9.7±1.1	A 1	S 30, Fe2+ 1	22
Balcom (1995)	11.9±1.8	A 1	S 30, Fe2+ 1	22
Baldock (1995)	12.5±1.1	Agar	S 50, Fe2+ 1, NaCl 1	5
Baldock (1995)	21.3±0.5	Agar	S 50, Fe2+ 1, NaCl 1	24
Rae (1996)	8.2±0.1	G 4	S 26, Fe2+ 0.2, BE 5	10
Rae (1996)	9.1±0.1	G 4	S 26, Fe2+ 0.2, BE 5, Fo 70	20
Rae (1996)	10.4±0.1	G 4	S 26, Fe2+ 0.2, BE 5, P 0.6	10
Rae (1996)	4.4±0.1	G 4	S 26, Fe2+ 0.2, BE 5, P 0.6	10
Rae (1996)	0.7±0.1	G 8	S 26, Fe2+ 0.2, BE 5, Fo 46	20
Rae (1996)	1.0±0.1	G 8	S 26, Fe2+ 0.2, BE 5, Fo 46, P 0.6	20
Rae (1996)	4.4±0.1	G 4	S 26, Fe2+ 0.2, BE 5, XO 0.2	10
Rae (1996)	6.5±0.1	G 4	S 26, Fe2+ 0.2, BE 5, BD 0.6	10
Rae (1996)	6.1±0.1	G 4	S 26, Fe2+ 0.2, BE 5, Fo 46, XO 0.2	20
Rae (1996)	6.3±0.1	G 4	S 26, Fe2+ 0.2, BE 5, AC 0.6	20
Rae (1996)	8.3±0.1	G 4	S 26, Fe2+ 0.2, BE 5	10
Kron (1997)	14±3	A 1.5	S 50, Fe2+ 0.5	22
Kron (1997)	20±5	A 1.5	S 100, Fe2+ 0.5	22
Kron (1997)	22	A 1.5	S 200, Fe2+ 0.5	22
Kron (1997)	11	A 1.5	S 50, XO 0.25	22
Kron (1997)	5±1	G 10	S 50 & 100, Fe2+ 0.5	22
Kron (1997)	9	A 1.5, G 3	S 50, Fe2+ 0.5	22
Kron (1997)	9	A 1, G2	S 200, Fe2+ 0.5, XO 0.2	22
Kron (1997)	3±1	A 1.5, G 3	S 50 & 100, Fe2+ 0.5, XO 0.1 & 0.25	22
Pedersen (1997)	14.6±0.1	G	S 50, Fe2+1.5, XO 1.5	-
Pedersen (1997)	8.1±0.1	G	S 50, Fe2+1.5, XO 1.5	-
Pedersen (1997)	8.2±0.1	G + BA	S 50, Fe2+1.5, XO 1.5, BE 5.0	-
Pedersen (1997)	17.8±0.2	A 1.5	S 50, Fe2+1.5, XO 1.5	-
Pedersen (1997)	16.3±0.2	A 3	S 50, Fe2+1.5, XO 1.5	-
Chu (2000)	1.4	PVA 20	S 50, Fe2+ 0.4, XO 0.4	20

Table 1-1 Fricke gel dosimeter ion diffusion measurements as observed in Baldock et al [35].Were : A = agar, agarose = agar, G = gelatin, PVA = polyvinyl alcohol, S = sulfuric acid H2 SO4 , XO = xylenol orange, BE = benzoic acid , Fo = formaldehyde, P = phenanthrol

From Eyadeh [67], the chemical reactions in the Fricke gels are shown in these equations:

$$H_2O \rightarrow H\bullet + OH\bullet$$

$$H\bullet + O_2 \rightarrow HO_2\bullet$$

Also, several other reactions occur in these chemicals that leads to the conversion of Fe^{2+} to Fe^{3+}:

$$Fe^{2+} + OH\bullet \rightarrow Fe^{3+} + OH^-$$

$$Fe^{2+} + HO_2 \rightarrow Fe^{3+} + HO_2-$$

$$HO_2- + H_3O+ \rightarrow H_2O_2 + H_2O$$

and

$$2Fe^{2+} + H_2O_2 \rightarrow 2Fe^{3+} + OH\bullet + OH^-$$

The Xylenol orange (XO) plays a significant role in measuring the signal of this mixture using spectroscopy in the visible range [66]. Also the ferric ions are not free to diffuse in the phantom due to XO [67]. As the ligand chelates of the XO leads to the colour change in the Fricke dosimeter [66]. Also, Liosi *et al.* [66] obtained four different complexes were found due to the irradiation of the Fricke dosimeter which then depend on the concentration of Fe^{3+} listed below:

$$3XO + Fe^{3+} \rightleftharpoons XO_3Fe$$

$$2XO_3Fe + Fe^{3+} \rightleftharpoons 3XO_2Fe$$

$$XO_2Fe + Fe^{3+} \rightleftharpoons 2XOFe$$

$$XOFe + Fe^{3+} \rightleftharpoons XOFe_2$$

Also, the change in the amount of ferric ions produced from the Fricke mixture depends on the energy absorbed by it, which is calculated using:

$$\Delta\,[Fe^{3+}] = \frac{D \times G(Fe^{3+}) \times\ 10\rho}{N_A \times\ e}$$

where D and G(Fe^{3+}) are the dose and the chemical yield of Fe^{3+} produced per 100 eV, respectively, and ρ is the mixture density, N_A is Avogadro number, and e is the number of Joules per electron volt.

1.2.3 Polymer Gel Dosimeters

In Alexander *et al*. [12], there was the development of polymer gel dosimeters. Two main changes happen when a polymer dosimeter is irradiated depending on the type of the polymer: degradation can occur in some polymers such as (polymethylmethacrylate); others like (polyethylene and polystyrene) can be cross-linked [13,14]. In, Oldham

et al. [15] a BANG3 gel was used with an approach where the 3D gel dosimeter was irradiated with IMRT treatment fields. The Resolution, Time, Accuracy and Precision criteria (RTAP) were applied when comparing the scanned gel to the expected distribution. These polymer gels were scanned with an optical CT system. On the other hand, when using MR gel-dose maps, it was observed that the accuracy dropped by five times. From Maryanski *et al.* [36], there was a development of a new dosimeter which was given the short name BANANA, which is bis, acrylamide, nitrous oxide and agarose. This mixture of gel dosimeter did not suffer from diffusion as the Fricke gel dosimeter had [36,37]. The significant drawback of polymer gel dosimeters was that their free radicals can interact with oxygen in the air thus it will prevent the polymerization process [28,37]. From Baldock *et al*. (1998) [38] and (1999) [39], this polymer gel dosimeter must be fabricated in an environment free of oxygen; it can be also fabricated in an environment that has nitrogen gas in it. From Baldock [28], normoxic gels dosimeters have helped in progressing gel dosimetry by using a new recipe of polymer gel dosimeters. The new recipe was known as MAGIC (methacrylic acid, ascorbic acid, gelatin and copper), the ascorbic acid works as an oxygen scavenger that helps in eliminating the oxygen from the gels.

1.2.4 Radiochromic Gel Dosimeters

As radiation therapy treatment methods have developed rapidly through the years, it has become necessary to develop new 3D dosimeter models. Radiochromic dosimeters are materials that change colour due to the absorbed energy from the radiation applied to it. This colouring is permanent and cannot be reversed [40]. The initial development was Fricke gel dosimeters in the 1950's with the addition of chemicals that change colour after being irradiated [11]. The fabrication of these Fricke dosimeters is easy and is not expensive, but they suffer from diffusion [11,27]. As a result, the development of a gel dosimeter with high sensitivity to radiation and less or the absence of diffusion would be significant addition to gel dosimeters.

In addition, a new 3D radiochromic gel dosimeter was presented by Adamovics and Maryanski [68] in 2003, known as (PRESAGE®) where they used leuco dye with polyurethane mixture and analysing it using optical CT. They obtained that the dose curve response was linear even in high doses of radiation. The down side is that the mechanical properties of this mixture dose not act as biological tissues.

The tool that is often used to read out the 3D dosimeters is MRI, but it is not always available for use. Hence, the need to develop other devices to be able to read the dose in these dosimeters. The development of optical CT scanners and optical spectroscopy really helped in improving the availability of 3D gel dosimetry [41].

From Andrew *et al*. [10], the development of a mixture of agar as a gelling agent with HCl to check if there was any change in the mixtures colour after radiation. From Armstrong *et al.* [42], they used the leuco Triarylmethane component which is colourless but when irradiated it changes colour.

1.2.5 F(B)X-type Radiochromic Dosimeters

The FBX dosimeter is consist of ferrous ammonium sulphates, benzoic acid and xylenol orange dissolved in sulphuric acid, it was developed by Gupta *et al.* [43,44]. From Gupta and Narayan [43], they developed a gel dosimeter known as FBX (ferrous ammonium sulphate, benzoic acid, and xylenol orange). The use of benzoic acid has helped in increasing the radiolytic oxidation of Fe^{2+} ions to Fe^{3+} ions with xylenol orange [43]. Also, xylenol orange helps to reduce the diffusion of the Fe^{3+} through the gel mixture [43,64].

1.3 Tissue-Mimicking Phantoms

Many tissue mimicking phantoms are being used in the medical imaging field to help in diagnosing and treating many illnesses, such as cancer, due to the similarity in their physical properties to several soft tissues in humans. These phantoms are used to help in many different aspects in the clinical industry, such as quality assurance, testing new approaches, and to compare different methods [16]. In the medical

field, there are many medical imaging approaches which are used in investigating and planning such as computed tomography, magnetic resonance imaging and ultrasound imaging. These various phantoms are growing and being developed rapidly by scientists in the last century, and they are very promising. The way that soft tissue is interacting with irradiation is fascinating to scientists and is leading the way to many other methods to be developed. There are different institutions that implement several guidelines for the machines used in radiation therapy such as: the Canadian Organization of Medical Physicists (COMP), the American Association of Physicists in Medicine (AAPM) and the American College of Radiology (ACR), that establishes the guidelines and specifications for various systems and applications [16].

Many tissue equivalent materials have been used such as gelatin, agar, and PVA. For every element, there are advantages and disadvantages. For gelatin the benefits are: it is easy to manufacture and it is not toxic.

Gelatin is one of the materials that have the same physical properties of human tissues and is widely used in the medical field. Also, gelatin is effortless to prepare and can be shaped into different models. Additives can also be added to the gelatin to have more stability in the fabricated gels, such as sorbitol and glycerol. Sorbitol, when mixed with gels, helps the refractive index (n) to be higher. As for the glycerol, when mixed with gels, it can help in keeping them more humid by maintaining the moisture inside it. The gelatin can be used as a

dosimeter by adding ferrous (Fe^{2+}) to the mixture. The radiation effect on the tissue can then be explored as the ferrous ions (Fe^{2+}) will change to ferric ions (Fe^{3+}) after irradiation. That will make xylenol orange in the gel change its colour due to the absorption of radiation. Tissue mimicking materials have been developed since the 1950's. From D'souza *et al.* [24], these phantoms were produced using agarose gel to mimic the prostate, fat and muscle tissue.

The materials were evaluated using MRI, US and CT, at room temperature of 22 degrees Celsius. For MRI, the relaxation times are the most important characteristics, the concentration of the agarose gel can highly affect the relaxation time T2. As for ultrasound, the attenuation and velocity are the most important characteristics. X-ray attenuation is the most important property of the computed tomography.

1.3.1 Definition of tissue mimicking material (TMM)

Tissue mimicking materials (TMM's) are materials that have the same physical properties of human tissue. So, these tissue equivalent materials act exactly as the human tissue when they are exposed to a force such as indentation or optical transmission. So, these TMM behave the same way the human tissue would under any force, heat and radiation. Also, these TMM's should have approximately the same density as the tissue they are mimicking. In addition, the 3% tolerance and 3 mm distance-to-agreement criteria should be used when

irradiating these phantoms to be able to calculate an acceptable dose [67]. It should be feasible to fabricate these TMM's into 3D phantoms to replicate the shape of the biological tissue.

1.3.2 Manufacturing

The process of preparing the tissue mimicking materials depends on the kind of the tissue we want to fabricate. When fabricating these tissues, the use of a gelling agent and distilled water, also some oils can be added to achieve a heterogeneous material such as breast tissue. Also, we can fabricate homogeneous materials such as lung by gelling agent and distilled water. From Oglat *et al.* [65] the need to fabricate a tissue mimicking phantom using different chemical materials such as:

1) Sigma silicon carbide (SC)

   It is a powder mixture of silicon and carbon, which can form ceramics. Also, it can be used in mimicking tissue materials to obtain the scatter properties by a backscatter factor.

2) Sigma aluminum oxide (Al_2O_3)

   The Aluminum oxide is also known as alkoxide, alundum, and alumina. It was used as a tissue mimicking material to study the attenuation and backscatter function.

3) Sigma konjac root glucomannan powder

   The konjac powder contains of water-soluble polysaccharide, it is used as a food thickener.

4) Sigma carrageenan powder for gel preparation

   The carrageenan also known as carrageenins is used in the food industry for its thickening, gelling, and stabilizing properties.

5) Sigma glycerol

   Glycerol is used in the pharmaceutical industry, as it is nontoxic odorless, and colourless. Also, the glycerol is used to investigates the acoustically.

6) Sigma gelatin

   Gelatin is a protein soluble in water, which can be produced in many concentrations. The use of gelatin as a tissue mimicking material in the medical field started with ultrasound imaging. The disadvantage of gelatin is its instability with temperature fluctuations.

Table 1-2 shows a summary of the chemicals used in tissue mimicking fabrication [65].

Material name	Manufacture	Main function
Water	Medical Physics Laboratory (USM)	To mimic the water concentration in the tissue
SC (400 grain)	Sigma-Aldrich	To modify the backscatter and allow it to mimic tissue
Aluminum oxide powder 3 µm	Sigma-Aldrich	To affect the attenuation, with a linear dependence as a function of frequency
Aluminum oxide powder 0.3 µm	Sigma-Aldrich	To affect the attenuation, with a linear dependence as a function of frequency
Konjac powder	11 Street Company	To mimic the human/animals tissue
Carrageenan powder for gel preparation (Type I)	Sigma-Aldrich	To mimic the human/animals tissue
Pc	Sigma-Aldrich	Used as a fertilizer for fertility the TMM
Glycerol	Sigma-Aldrich	To provide the required speed of sound

Table 1-2 A summary of the chemicals used to fabricate tissue mimicking materials. TMM:Tissue mimicking material, SC: Silicon chloride, Pc: Potassium chloride [65].

1.3.3 Application of Gelatin as Tissue-Mimicking Material

These tissue mimicking materials are applied in many different applications in life since 1950s. One of the applications these phantoms are developed for is as a radiation dosimeter. Also, it is used as a model in some cancer treatments such as hyperthermia, which is used to kill or make the cancer cells weak by heating them [29]. In addition, the tissue equivalent materials can be used to fabricate breast tissue and shape to help the physicians in there training to take a biopsy from the affected tissue [30]. The tissue equivalent materials are used to check the effects and performance of these applications on the human body and tissue, such as wearable antennas for body area network (BAN)

[45]. Also, these TMMs are used to measure the electromagnetic energy from the mobile terminals [46].

1.3.4 Simulation of Lungs

The human lung is occupied with air bubbles in them and also has some solid tissue such as lobes, bronchus and tracheal wall.

The human lungs are located in the thoracic cavity and is enclosed within the rib cage [70]. In Figure 1-2 is the gross anatomy of the human lungs, where each lung is inside the pleura [70].

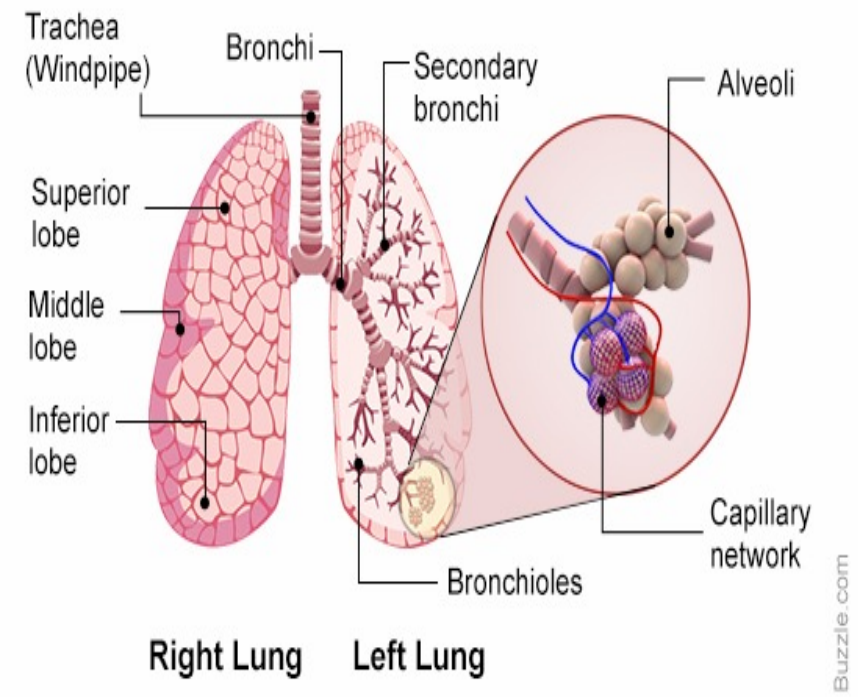

Figure 1-2 The gross anatomy of the human lungs [70].

Each lung in divided into different segments called lobes through partitions called interlobar fissures. The right lung has three lobes which are: superior lobe, middle lobe, and inferior lobe. As for the left lung the it is slightly smaller than the right lung and has two lobes known as the superior and inferior lobes. The bronchi are made from the hyaline cartilage and smooth muscles, and they connect the lungs with the nasal and oral cavities. Also, the bronchi branches inside the lungs to the secondary bronchi, then they will give rise to bronchioles. These bronchioles end into very small inflatable sacs or bags named alveoli, were air is exchange between the lungs and blood. So, when whisking our gelatin mixture to achieve a low density phantom due to the air bubbles in the mixture. Which replicates the inflatable bags in the lungs [70].

The fabrication of a lung using TMM with gelatin as a gelling agent can be done in different ways. From Borges *et al.* [26], the manufacturing of a lung can be achieved by adding some Styrofoam beads to the 300 bloom gelatin mixture. These beads are in different sizes, which helps in achieving different densities. So, the density of the gel mixture is obtained from the density of the forming material and the bead's density, and is given in this equation:

$$\rho_{cell} = 0.74\,\rho_{be} + 0.26\,\rho_{int}$$

where ρ_{cell} , ρ_{be} , ρ_{int} are the densities of the gel mixture, beads and the forming material, respectively [26].

The achieved mixture density was 0.28 g/cm^3 and it is approximately the same as a human lung which has a density of around 0.3 g/cm^3 [26].

Also, Olberg *et al.* [47], the 5% 300 bloom gelatin mixture was whisked for 2 minutes to obtain a foam, thus to achieve a low density mixture. From Adams *et al.* [49], the Hounsfield number (HU) of the lung is between -770 HU - -875 HU, and the Hounsfield number that was found by (Olberg et al 2000) is – 600 HU for the low density foam. In addition, De Deene *et al*. [48] the 12% concentrated 300 bloom gelatin mixture was beaten with a kitchen mixer to achieve a foam. The foam density that was achieved was between 0.25 - 0.35 g/cm^3, which is approximately equivalent to a human lung density [48].

The importance of replicating a lung is to use the phantom to perform quality assurance to verify the accuracy of dose delivery in low density tissues.

1.4 Gelatin

1.4.1 History

Gelatin is known to be used in making a delicious treat with a popular name (Jell-o) [17]. It is used in the food industry for a long time and is manufactured from the bones, connective tissues, and skin of many different animals, such as but not limited to, cows, fish, and pigs.

Gelatin comes in various forms such as powder and sheets. These forms are soluble in high-temperature water where it gives more than five times its original volume [32]. Also, the gelatin is odourless, tasteless and colourless, which helps in manufacturing a transparent phantom. The gelatin is a high protein source that contains collagen. Gelatin is soluble in water but in some cases the need to use heat to enhance its solubility [17]. Therefore, we will have a clear solution. From the GMIA handbook [22], the gelatin is produced from the hydrolysis of the collagen that can be found in the vertebras, skin, and bones. The gelatin itself is an animal-based. As for the vegetable gelatin (agarose), which is extracted from seaweeds, the chemical relation is not known. Due to the two different extraction methods type A and B gelatin has been obtained.

Type A gelatin is extracted using acid; type B gelatin is extracted using an alkali procedure. Figure 1-3 shows the process of deriving the gelatin from the animal's bones and skin.

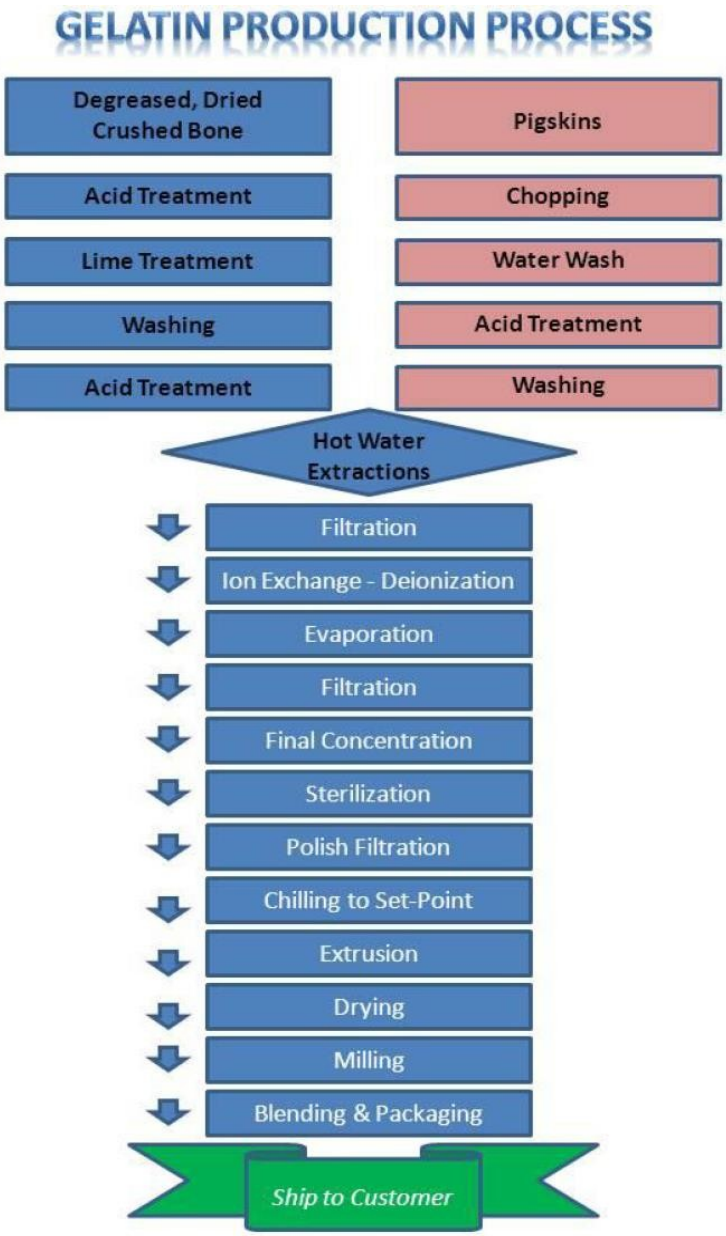

Figure 1-3 : The gelatin production process from the GMIA handbook [22].

Gelatin is a combination of several elements which are: carbon, hydrogen nitrogen and oxygen with 50.5%, 6.8%, 17% and 25.2%,

respectively. Gelatin has a relative density of 1.4, and the moisture content is between 8-13%. It is soluble in water, acids and insoluble in chemicals with hydrocarbons bond such as benzene, methanol, ethanol, and acetone. Due to the hydrolysis of the gelatin, many amino acids can be obtained as seen in (table 1-2).

	Type A (Porkskin)		Type B (Calf Skin)		Type B (Bone)	
Alanine	8.6	10.7	9.3	11.0	10.1	14.2
Arginine	8.3	9.1	8.55	8.8	5.0	9.0
Aspartic Acid	6.2	6.7	6.6	6.9	4.6	6.7
Cystine	0.1		Trace		Trace	
Glutamic Acid	11.3	11.7	11.1	11.4	8.5	11.6
Glycine	26.4	30.5	26.9	27.5	24.5	28.8
Histidine	0.9	1.0	0.74	0.8	0.4	0.7
Hydroxylysine	1.0		0.91	1.2	0.7	0.9
Hydroxyproline	13.5		14.0	14.5	11.9	13.4
Isoleucine	1.4		1.7	1.8	1.3	1.5
Leucine	3.1	3.3	3.1	3.4	2.8	3.5
Lysine	4.1	5.2	4.5	4.6	2.1	4.4
Methionine	0.8	0.9	0.8	0.9	0.0	0.6
Phenylalanine	2.1	2.6	2.2	2.5	1.3	2.5
Proline	16.2	18.0	14.8	16.4	13.5	15.5
Serine	2.9	4.1	3.2	4.2	3.4	3.8
Threonine	2.2		2.2		2.0	2.4
Tyrosine	0.4	0.9	0.2	1.0	0.0	0.2
Valine	2.5	2.8	2.6	3.4	2.4	3.0

Table 1-3 The amino acid obtained after the hydrolysis of the gelatin [22].

Furthermore, the gelatin can be stored for a long time when it is kept in a sealed case. The gel strength (bloom) and viscosity are the essential characteristics. The bloom of gelatin is determined using an indentation test (the bloom test), where the bloom is the mass in grams required to depress the surface of the gel by 4mm.

The gelatin bloom is between 25 to 325. Lower strength is known as low bloom; higher strength is known as high bloom. Due to bloom intensity, the use of less concentration of gelatin is possible. Also, the gelatin increases its strength while time passes as seen in (Figure 1-4).

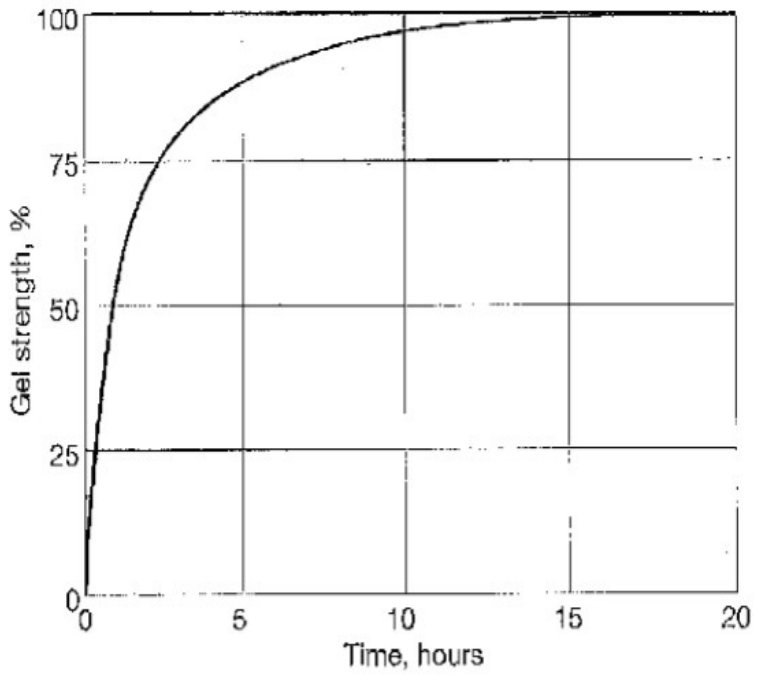

Figure 1-4 : The effect of time on the gelatin strength of a 6 2/3% gel at 10 ˚C [22].

As can be seen in (Figure 1-5), the gelatin concentration increases when the gelatin bloom increase. So, the relationship between them is directly proportional.

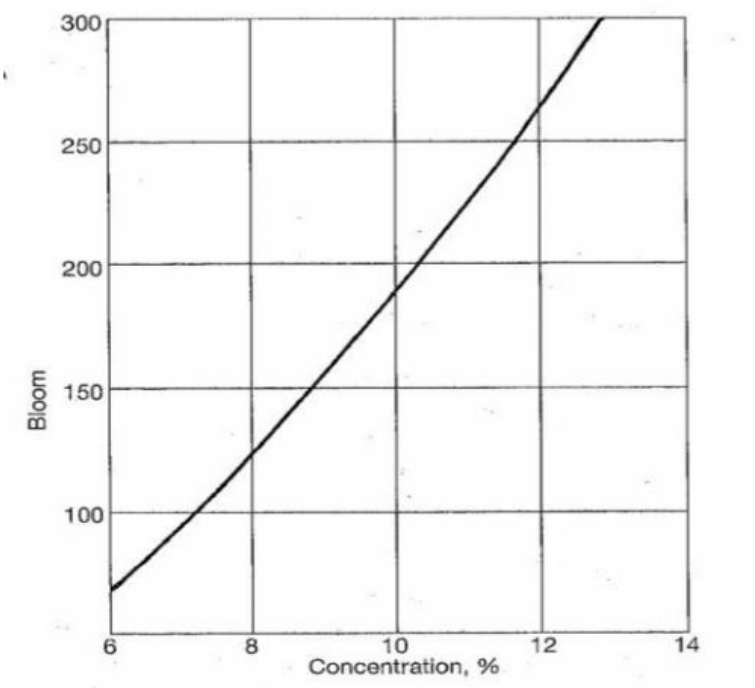

Figure 1-5 : The effect of bloom on the gel concentration at 10 ˚C [22]

As for the viscosity of the flow time of 100 mL of 6.67% under a temperature of 60 degrees Celsius. The (Figure 1-6) shows how the viscosity reads with various gelatin blooms.

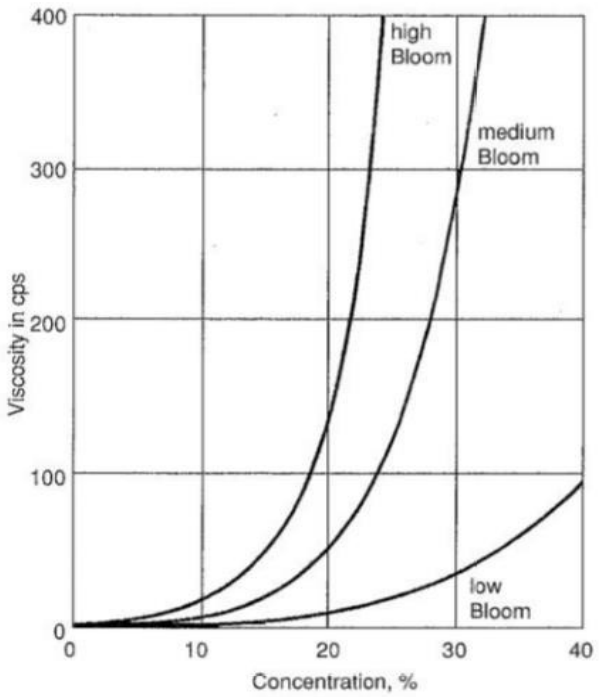

Figure 1-6 : The effect of gelatin concentration at 60 ˚C on the viscosity which has a unit of centipoise (cps) [22].

Also, by adding some sorbitol, glycerol and water to the gelatin mixture will help in the increase of light refractive index that will help the light to transmit in the mixture and will keep the gel from drying. The stability of the gelatin depends on the bloom of the gelatin, which has different ranges. The higher the bloom number, the stiffer is the gelatin.

1.4.2 Elastic Properties

The elastic properties of gels are fundamental in the pharmaceutical industry primarily when used in medicine fabrication, food industry manufacturing, and in biological engineering. The elastic modulus can be used to assess these soft materials only to a certain point. This modulus is linear when used with more rigid materials, not soft tissues. Therefore, stress, strain, and the indentation are the most suitable metrics for tissue- mimicking substances. The indentation test is clear to understand and to achieve. The elastic properties are significantly important when using TMM's in radiation therapy as it helps us in fabricating a phantom with similar properties of biological tissue.

The indentation test is to apply force on a material and analyse how does it affects it. That can be done in many scales such as Nano and Micro, where Nano indentation and Micro indentation are the use of small loads and indenter tip on micrometer or nanometer area, as these tests can measure the hardness of these materials.

The Nano- indentation is best to be used when the soft tissue is heterogenetic, as the Nano-indenter is precise and can offer accurate results [53]. The Micro- indentation is helpful, especially in food manufacturing as it can estimate with high accuracy their quality [53]. As for gels, the bloom test is the most common test to determine the stiffness of the gels, the higher the gel blooms, the stiffer these gels will be. The elasticity of materials is the ability of these materials to return to their original state after the force applied on them is removed. From Gregoric [60], the experimental approaches to quantify the mechanical properties of homogeneous phantoms is by applying the stress and strain modulus that appeared to have a linear change. The shear modulus of these gels has been shown to depend on the concentration of the protein that is in these gels. Even at low concentrations of these proteins, the elastic modulus is still linear [60].

1.4.3 Low Density Foams

From GMIA handbook [22], gelatin has a relative density of 1.3 - 1.4 g/cm^3, so to be able to achieve gels with lower density there are many approaches that could be implemented. From Lambert *et al*. [31], the resorcinol formaldehyde aerogel was used to achieve a low-density foam by reducing the freezing time to minutes rather than hours. The density of the 2mm shells that were produced was near 0.05 g/cm^3. Also, from Kim *et al.* [32], they fabricated a foam using gelatin and the mixture of gelatin and hydroxyapatite in different concentrations. The

gelatin was mixed for 1 hour at a 40 ℃, then poured into a container that was placed into the freezer for a day at a temperature of -20 ℃. The gel was then cryodesiccated for 3 days to form a sponge. They achieved a density of 0.056 g / cm^3 [32]. As for the mixture of the gelatin and hydroxyapatite it was fabricated in two concentrations: 10% and 30%. It was mixed for 6 hours and then frozen for 24 hours at -20 ℃ then cryodesiccated for 3 days. It was then crosslinked and vacuum-dried for 2 days [32]. They achieved a density of 0.102 and 0.182 g/ cm^3 for 10% and 30%, respectively [32]. From Salerno *et al.* [50], they used zein and gelatin as gelling agents and they were foamed using the gas mixture of Carbon (CO_2) and Nitrogen (N_2), achieving a density of 0.1 g /cm^3. In addition, Halberstadt *et al.* [51] achieved a low density foam equal or under 0.32 g / cm^3 by using santoprene material and foaming it using a foaming agent such as, but not limited to, liquid CO_2 and hydrocarbons.

1.5 Measurement of Elastic Properties

The measurement of the mechanical properties of materials such as elastic properties by implementing indentation method was known since the 1970's [55-56]. These methods were widely investigated by many such as Doerner *et al.* [57], Loubet *et al.* [59] and Oliver *et al.* [58]. The elastic properties of any materials are very important and can be obtained by different modulus such as, but not limited to, Young's modulus, shear modulus, and the bulk modulus. Where the Young

modulus is the measurement of the ability of a material to resist changes in length when a force is applied to it. As for the Shear modulus it is the numerical constant that explains the elastic properties of solids when a force applied on it. The Bulk modulus is how much a material will compress when an external pressure is applied on it.

Also, this modulus is correlated with the stiffness of the material, and the ability of the material to resist deformation. To evaluate these properties, several methods may be used such as but not restricted to, indentation and needle penetration.

1.5.1 Indentation

The elastic properties of soft materials can be obtained by applying some force on these soft materials. The use of indentation is a well established technique to quantify stiffness. The indentation method is done by using different indenter geometries, such as but not limited to spherical, flat sided and cone shaped. Long *et al.* [52], investigated how gel phantoms can react when indented. The microscopic indentation procedure was implemented on the gel phantoms to measure the Young's modulus, which is obtained from the force placed on the gels and the depth of the indenter rod. The Young modulus was calculated using Hertz theory and it was noticed that there was incompatibility in between the Young modulus obtained and the different gel thickness from the same mixture. Therefore, the need to add a correction factor to these results was essential. Marina *et al.* [53]

investigated the elastic modulus of hydrogels using different methods of indentation. They used a spherical and a flat side indenter in the Nano and Micro scale to determine the elastic properties of the hydrogel rather than using bending and/or tensile tests, as these gels are soft and can break easily. After performing these indentations they showed that the elastic modulus determined by Micro indentation of the hydrogels was linear for the flat end indenter, as for the spherical indenter the elastic modulus was found to be non-linear [53]. When using the Nano indenter, the elastic modulus was found to be linear and the change in the shape of the gels was not significant [53]. David *et al*. [54] used Atomic Force Microscopy (AFM) on PVA gels and biological tissues to obtain the elastic properties of these materials.

Therefore, we can conclude that the use of indentation methods with several indenter shapes is easy to implement and can help to obtain the mechanical properties of these soft materials by analysing them using well established models.

1.5.2 Needle Penetration

The measurement of elastic modulus of soft materials such as gel phantoms can be achieved by the use of methods such as indentation, which was discussed in the previous section. In addition, the elastic modulus can be obtained by needle penetration. From Vieira *et al.* [30], they fabricated a paraffin gel as a tissue mimicking material (TMM) and embedded a sold mass into the breast phantom. The main purpose

of this breast phantom was to train physicians to perform a certain biopsy procedure [30]. The needle was used to obtain the elastic properties of breast phantoms fabricated with two different densities: high density tissue (HDT), which is the embedded solid mass, and medium density tissue (MDT), which represents the breast tissue. From Okamura *et al.* [61], they used a puncture force by the needle to determine the stiffness of these soft tissues, as the stiffness is linked directly to the elastic properties of these soft tissues. The elastic properties are linear when we have small deformation in these tissues, but when the deformations are large then the change would be non-linear and we need to use a different modulus to fit these data [61]. From Roesthuis *et al.* [62], the needle interaction with soft tissue is subject to two forces: the force of friction when the needle touches the surface and the force needed to the needle to be injected in the soft tissue. A gelatin phantom was used to test the puncture of the needle into the phantom, which will help in obtaining the force of friction and insertion force to measure the firmness of the gelatin phantom [62]. From Duriez *et al.* [63], the use of needle penetration in soft materials can help obtain the elastic properties of these soft tissues. The needle can go through this soft tissue for a large depth with a small change in the shape of that phantom. Thus, for small deformations, the Hook's law, Poisson ratio, and Rayleigh model can be used to model these soft tissues [63]. Where Poisson ratio is the negative ratio of the transverse contraction strain to the longitudinal extension strain. As for the Rayleigh model is a special case of the Weibull distribution when m=2,

where the cumulative defect arrival pattern (CDF) and the defect density over time (PDF) is calculated using:

$$CDF: F(t) = 1 - e^{-(t/c)^2}$$

$$PDF: f(t) = \frac{2}{t}\left(\frac{t}{c}\right)^2 e^{-(t/c)^2}$$

Where t and c are the time and scale parameter, respectively. As the scale parameter is a function of t_m the time when the curve reaches its peak [69].

1.6 Optical Transmission Measurements

The optical transmission measurements can be obtained after the irradiated FXO gels change colour to dark orange (eventually purple when saturated by Fe^{3+}) with an absorption peak at 589 nm. From this absorption peak the linear attenuation coefficient (μ) is obtained for all of the irradiated gels and for the background gels (unirradiated gels). The absorbance or optical density (OD) of these gels is obtained using Beer-Lambert Law:

$$A = OD = -Log_{10}\left(\frac{I_{irradiated}}{I_{unirradiated}}\right)$$

The above equation is correct in the absence of scattering. The optical density is the total attenuation, which may include the scattering and

reflection of the incident light. So, if the scattering and/or reflection was taken into consideration then the above equation will overestimate the absorbance.

This research was done in three stages: the first stage was to obtain the mechanical properties of the tissue mimicking material (TMM); the second stage was to fabricate a radiochromic gel slabs; and the last stage was to measure the absorbed dose in these slabs using a spectrometer, where these slabs could be used as a quality assurance tool.

1.6.1 Optical Properties

The light is known to be an electromagnetic (EM) wave. The visible range falls between 400-750 nm (Figure 1-7).

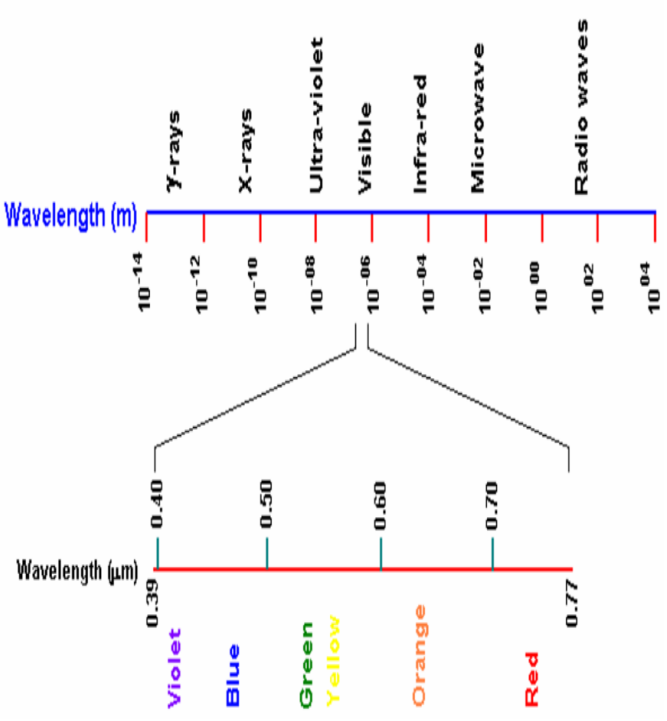

Figure 1-7: Electromagnetic wave spectrum [33].

The optical properties depend on the materials that the light will interact with. Materials are classified to three categories:

1) Transparent materials.
2) Translucent materials.
3) Opaque materials.

The opaque materials do not allow the light to transfer through them such as metals [33]. Metals can transmit high energy like gamma-ray (γ) and X-ray, as the high energy photons have a high frequency. Hence, the visible light has a low frequency thus cannot be transmitted through the opaque's materials [33].

1.6.2 Optical Transmission

The optical transmission is one of the properties discussed in section 1.6.1. When the light transmits through a tissue mimicking material, there will be numerous interactions such as; scattering, reflection and absorption Figure 1-8. To be able to obtain a quantity related to these properties, we need to calculate the absorption coefficient μ_a (cm^{-1}) and the scattering coefficient μ_s (cm^{-1}). The absorption coefficient μ_a is the fraction of energy absorbed per unit path length, as for the scattering coefficient μ_s it is the fraction of energy scattered per unit path length.

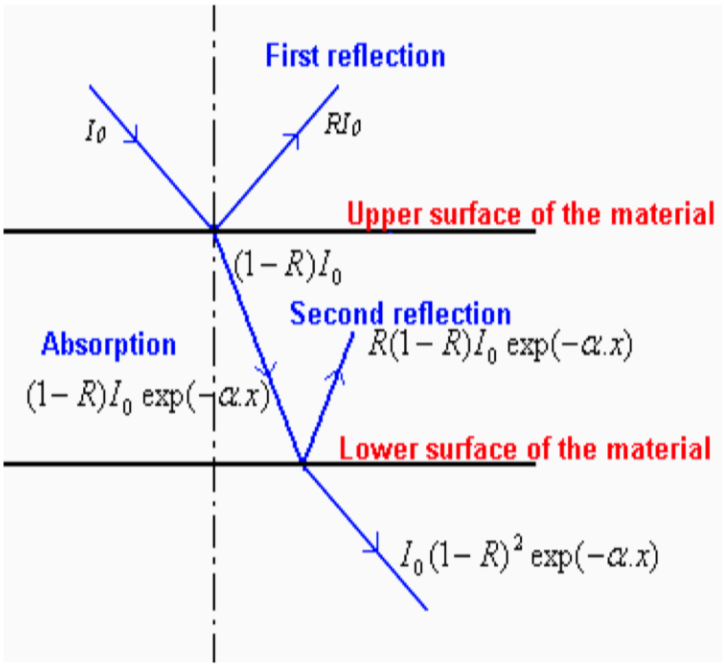

Figure 1-8 The course of light transmission through a material [33].

Hence, the chemical and physical characteristics of these tissue mimicking materials (TMM's) have a significant effect on how light interact with these phantoms [16]. By examining the transmission of light through the tissue phantoms relative to a reference we may obtain the absorption spectrum of the chromophores within.

1.6.3 Effect of Scattering on Light Transmission Through a Slab

When light goes through a material many interactions occur: one of them is scattering. It can be described by the scattering coefficient μ_s. The scattering of light was known since 1871 and was defined by Lord Rayleigh.

Therefore, the more light scatters through any medium the less the amount of light transmitted through that medium.

So as can be seen from the equation the intensity of the transmitted light is changing exponential with the thickness of the slab, the thicker the slab is the weaker the transmitted light is. This is assuming there is no scattering, but if light scatter was not neglected then the Beer-Lambert equation will be

$$I = I_\circ e^{-(\mu_a+\mu_s)x}$$

where $\mu_a \; and \; \mu_s$ are the absorbance coefficient and scattering coefficient, respectively, *I* and $I_\circ$ are the transmitted and instance light intensity, respectively, and x is the materials thickness. Thus, when not accounting for the scattering coefficient that will lead to overestimate the absorbance coefficient.

1.7 Thesis Proposal

In this research the goal is to fabricate a phantom that replicate the density of human lung, which is between 0.25 – 0.35 g/cm^3. Many different processes have been implemented by others to achieve the desired density, such as adding Styrofoam beads in the polymer gelatin mixture. Another option, our chosen approach, is to create a gelatin foam. We will then dope the foams with radiochromic chemicals, FXO in this study, to investigate the dose response. Measurements of optical transmission will be correlated to the delivered dose.

2. Methods and Materials

2.1 Gelatin Fabrication

The preparation of gelatin was done in four different percentages by weight: 5%, 10%, 15%, and 20%. Also, two strengths of gelatin were used, which were 220 bloom (bulk food-grade gelatin) and 300 bloom from (Sigma-Aldrich, St. Louis, USA). So, we were able to prepare two batches of gelatin with different blooms and fractions. When preparing the gelatin, we start by heating the distilled water to 50 degree Celsius then the gelatin powder was poured into the water gradually and mixed until all the powder dissolved Table 2-1 summarizes the preparations of the 220 and 300 Bloom gelatins. The main problem when fabricating the gels is making sure the powder completely dissolves so we will not have any clumps in the mixture. We should not whisk the mixture too much, to avoid introducing any air bubbles in the gels. After that, the mixture is poured into ice cube trays. Each cube contains 50 mL of the mixture. The trays are covered with plastic wrap to prevent the gelatin cubes from drying. The cubes were left in the fridge to set for 24 hours. After the gels have set, it was noticed that the 5% gelatin were unstable, so they were excluded from the indentation experiments.

Gelatin %	Gelatin (g)	Distilled water (mL)
5	20	400
10	20	200
15	20	133.3
20	20	100

Table 2-1 Gelatin preparation in different concentrations.

2.1.1 Gelatin Indentation

The indentation apparatus consisted of a probe that was tipped with a sphere of a diameter 6 mm. The gel cubes were put on a flat surface under the indenter rod as seen in (Figure 2-1). Then, a mass ("major force") is placed on the weight platform and the reading recorded from the dial (mm). The masses used were 100, 150, 200, 250, 300, 500 g. When applying the major force to the weight platform, caution was taken that the rod did not penetrate the surface of the gel. It should also be noted that when indenting the gelatin cubes we focused on the middle areas away from the sides to minimize any errors due to the edges. A total of 20 indentations per major force for every gel concentration were taken, and the average and the standard deviation of each depth was calculated.

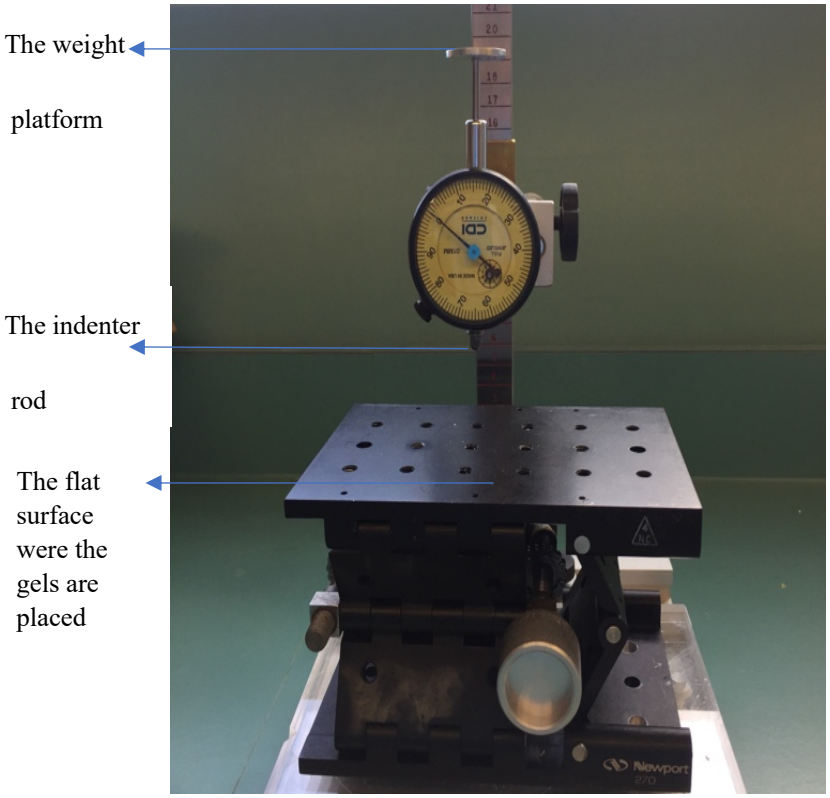

Figure 2-1: The apparatus used in finding the mechanical properties of gels and foamed gels.

2.2 Gelatin Foam Fabrication

The gelatin foam was prepared by the 300-bloom type A gelatin from (Sigma-Aldrich, St. Louis, USA), and the 220-bloom gelatin (food-grade gelatin). These two gelatin blooms were used at a concentration of 15%, with the addition of some sorbitol and glycerol. The process of generating gelatin illustrated in Table 2-1 then the sorbitol alone was added to the gelatin mixture by different concentrations: 1%, 3%, and 5%. The mixture was whisked by a kitchen mixer on high speed for 1, 2, 3 and 5 minutes. Afterward, the foams were placed in a cube tray in

the refrigerator for 12 hours. The same technique was applied to another batch of 15% gelatin, both 300 and 220 bloom but with a different percentage of glycerol alone: 1%, 3%, and 5%. These samples were also set for 12 hours in a fridge. A final batch of gelatin was made by adding both the sorbitol and the glycerol in different concentrations (Table 2-2). These foamed samples were frothed for 30, 90, 180, and 300 seconds.

Substance percentages %	Sorbitol (g)	Glycerol(g)
1	1.5	1.5
3	4	4
5	7	7

Table 2-2 The different concentration of sorbitol and glycerol added to the gelatin.

2.2.1 Gelatin Foam Indentation

Foams were allowed to set for at least 12 hours in the fridge prior to indentation. The gelatin foams were placed under the indenter rod on a flat surface, and the major force was applied carefully to ensure the sample was not damaged.

Afterward, the reading on the dial was noted then the same procedure was repeated 20 times at different locations around the foams surface.

The masses that were used were 100, 150, 200, 250, 300, and 500 g. The gelatin foam that was used comprised three batches of different mixtures where were (gelatin with sorbitol, gelatin with glycerol and gelatin with both sorbitol and glycerol). In total there were six batches of foamed gelatin due to the use of two different blooms of gelatin (220, and 300 bloom).

2.2.2 Gelatin Foam CT Scan

Independent batches of gelatin foam were prepared as mentioned in section 2.2 with different frothing times. The gelatin foam cubes were scanned using Computed Tomography (CT). The gelatin foams were left in the silicon tray and placed on the CT bed. Then, the cubes were scanned, and the data and pictures were sent to the Pinnacle treatment planning system for analysis. Volumes of interest were contoured and the CT statistics recorded. CT number was subsequently converted to density using the default conversion table. It was found that the 180 and 300 seconds of frothing had approximately the same density as the human lung which was 0.33 ± 0.16, and 0.33 ± 0.052 g/cm^3, respectively.

2.3 Ferrous-Xylenol Orange (FXO) Gel Fabrication

The Ferrous-Xylenol orange gel was prepared as explained in [23] using 10% by weight of 300 bloom gelatin from sigma dissolving it in 90% by weight of Sulfuric acid (H_2SO_4). The Sulfuric acid (H_2SO_4) was obtained from a 50 mM stock solution that was diluted from a concentration of 98% (Sigma-Aldrich). The 50 mM H_2SO_4 is heated using the hot plate to achieve a 60-80 ^oC, then the gelatin is poured into the solution gradually and stirred until completely dissolved, making sure to not have any bubbles in the mixture. After that, the mixture is left to cool down to a temperature of 30-35 ^oC. Then as illustrated in [23], the Fe^{2+} and the XO were added in these amounts (0.3 mM and 0.05 mM), respectively. The mixture was then blended until it all dissolved completely. The mixture was kept below 30-35 $^\circ C$ due to the auto oxidation of Fe^{2+} to Fe^{3+} when added at higher temperatures. The mixture was poured into 5 mm thick sheet moulds as seen in (Figure 2-2), making sure no bubbles formed in the gelatin mixture. The filled moulds were stored in the refrigerator overnight. Another two batches of the same mixture of gelatin 300 bloom (Sigma Aldrich) and Fe^{2+} + XO were whisked using a hand mixer on high speed for 2 minutes and for 5 minutes and then poured into sheet moulds and refrigerated overnight. Pouring the whisked mixture was done rapidly, as the foamed mixture tended to stick to the container that it was frothed in. It should be noted that, when preparing the foamed gelatin + FXO

mixture, it should be done one at a time. Table 2-3 summarizes the FXO gel preparation concentrations.

Gelatin by weight	50 mM of H_2So_4	Fe^{2+} mM	XO mM
10%	90%	0.3	0.05

Table 2-3 The FXO gels preparation method.

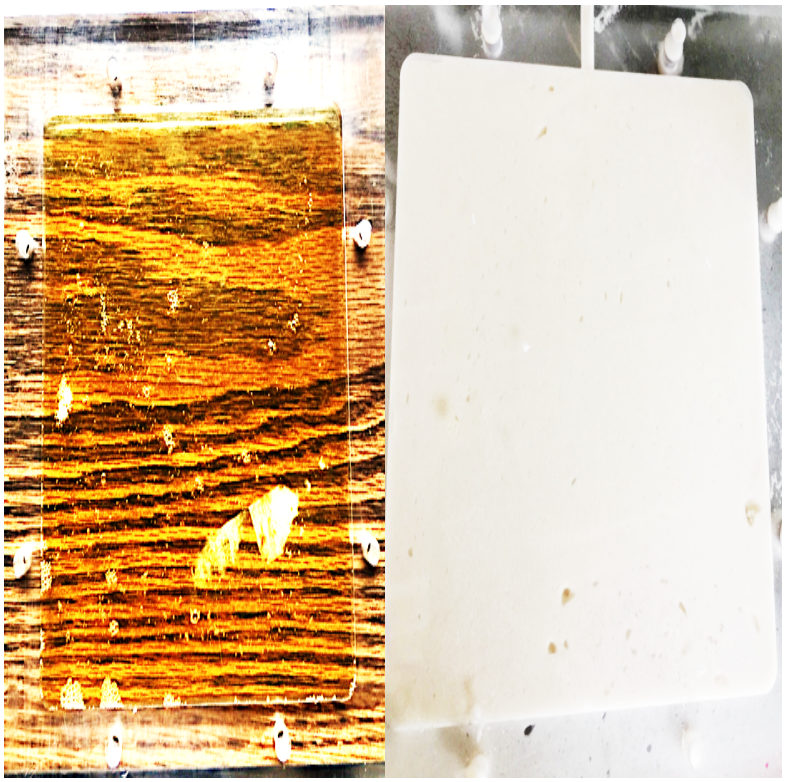

Figure 2-2: The left picture is the FXO gelatin thin sheet, as for the right one it is the foamed FXO gelatin.

The next day, the sheets were taken out of the plastic plates and were cut into four squares and placed inside a plastic bag to hold the moisture in them and keep them from drying. There were a total of eight squares of each formulation. Two of these squares were reserved as unirradiated reference samples.

These square sheets were taken out of the refrigerator 30 minutes before irradiation to be at room temperature. The samples were irradiated using a LINAC by delivering 100, 200, 400, 600, 800, 1000 MUs. The sheets were sandwiched between 5.2 cm of polystyrene while being irradiated with a 6 MV, 10 x 10 cm^2 field. The mid-plane of the samples was located at the isocentre plane, and centred within the light field. It was approximated that each Monitor unit (MU) delivered to these sheets is corresponded to 1 cGy. After the irradiation the sheets changed their colour from yellowish orange to shades of brown and purple, due to the change of Fe^{2+} to Fe^{3+}, as can be seen in Figure 2-3.

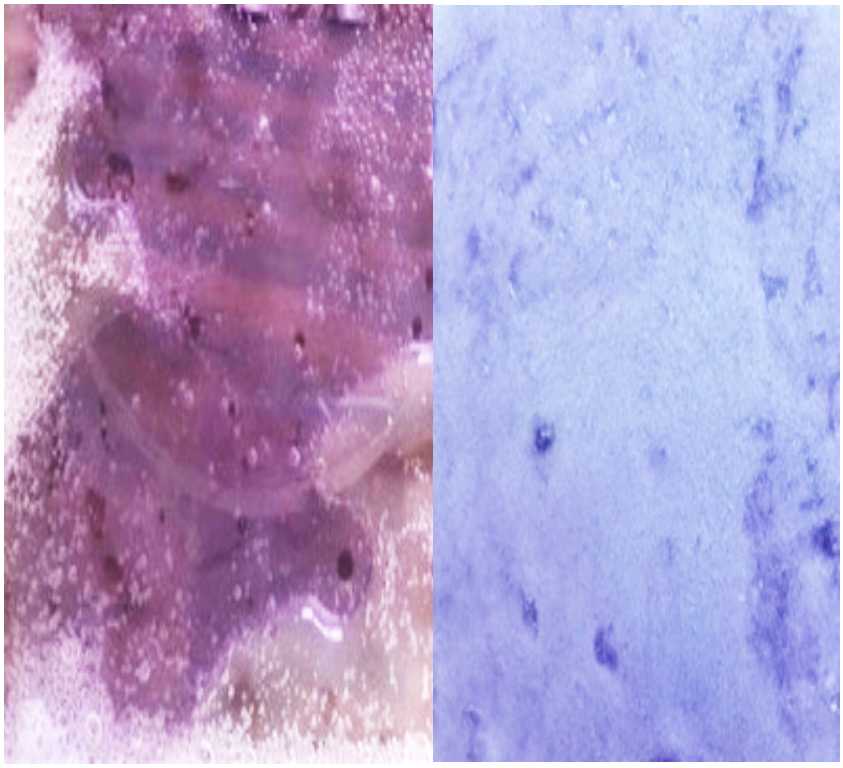

Figure 2-3: The left picture is for the gel FXO after irradiation, as the picture on the right is for the foamed gel FXO after irradiation.

The post-irradiation colour changes were quantified using a simple transmission measurement to obtain the change in the total attenuation coefficient spectra with the apparatus shown in Figure 2-4. The measured transmission through the irradiated sheets was referenced to the transmission through the unirradiated samples. Spectra were collected using an Ocean Optics HR4000 spectrometer paired with a broad band quartz-tungsten-halogen (QTH) light source.

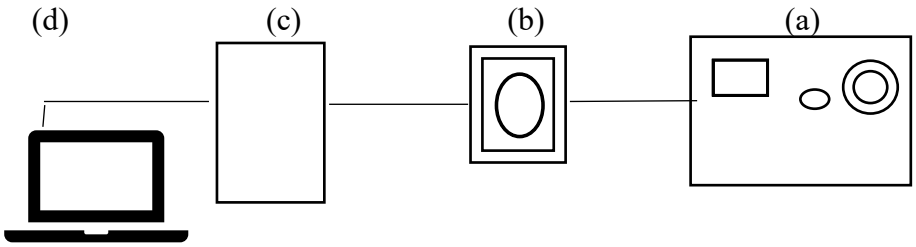

Figure 2-4 A sketch of the linear spectroscopy apparatus. Where (a) is the fiber optic llluminator device, (b) is the plastic holder that holds the gelatin sheet with a window in the middle, (c) is the Ocean Optics spectrometer (HR4000), (d) the computer that hold the Ocean View analysis system.

To be able to obtain the absorbed dose in these thin FXO slabs by the yellow light fiber optic, which can be delivered with different intensities, thus the light will interact with the thin sheets through the plastic holder window. Many interactions can occur between the light and the FXO sheets, such as absorbance, refraction and transmission. The measurements were collected using software from Ocean Optics and the spectra processed and analyzed in Microsoft Excel.

3. Elastic and Radiological Properties of Gelatin

As we discussed in (section 1.4.2), the elastic properties of gelatin are essential to the production of medications, foods and in tissue engineering. The elasticity of these materials gives them the ability to return to the original shape after applying force to it. The elastic properties of gelatin can be represented by the Young modulus, which is linear with rigid materials; as for soft materials, it is linear to a point then it decreases. The best modulus to evaluate the soft materials would be the stress-strain modulus, measured using Micro or Nano indentation techniques. Gelatin stiffness is best measured using the bloom test, where the relationship between the stiffness and the bloom of the gelatin is directly proportional.

We implemented a standard indentation test on the gelatin cubes which were fabricated as described in (section 2.1). The samples were placed under the indenter as shown in (Figure 2-1). The mechanical properties of the gelatin cubes were determined from the compressibility, that is the indentation depth (mm) that resulted from a major force (g). When applying this major force on the 220 bloom cubes, it was found that the higher the gelatin concentration the indentation depth decreased, thus the need of heavier weight (larger force) to achieve same change in depth. The same procedure was done with the 300 bloom gelatin, where it was fabricated as described in (section 2.1). The indentation test was also performed on them. For both the 220 and 300 bloom

gelatin, the relation between force (g) and the indentation depth (mm) was linear as the gelatin cubes are acting as elastic materials. As seen in Figure 3-1 the effects of the force by grams (g) on the depth (mm) in these gelatin cubes should be linear, which was expected due to the elastic behaviour of these materials. As shown in Figure 3-1, the higher the concentration of the 220 bloom gelatin the lower the indentation depth is, a result of the stiffness of the gelatin cubes which indicates an inverse relationship between the depth and the gelatin concentration.

Figure 3-1 The effect of force on different concentrations of 220 bloom gelatin cubes in a line graph

The indentation measurements were also performed on gelatin cubes manufactured using 300 bloom gelatin. These samples were produced using the same gelatin concentration to facilitate comparisons. The data are shown in Figure 3-2 .

Similar to the 220 bloom measurements, the indentation depth of the 300 bloom gelatin cubes changed linearly with the applied major force.

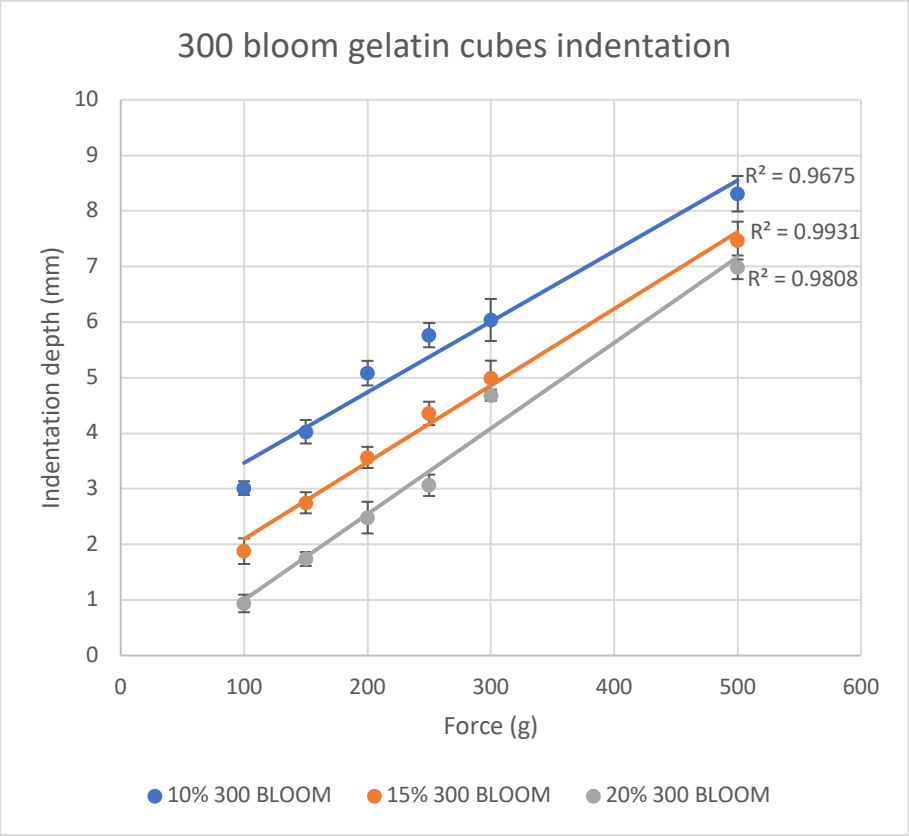

Figure 3-2 the effect of force on different concentrations of 300 bloom gelatin in a line graph..

As for the foamed gelatin cubes the indentation process was done the same way as the un-foamed. Six batches of foamed gelatin with sorbitol, glycerol and the both sorbitol and glycerol in 220 and 300

bloom gelatin were prepared. The indentation change in these cube sets is shown in Figure 3-3, Figure 3-4, and Figure 3-5, for the sorbitol gelatin foam, glycerol gelatin foam, and both sorbitol and glycerol gelatin foam cubes, respectively. In these Figures a positive correlation between the applied force and the indentation depth was observed.

(a)

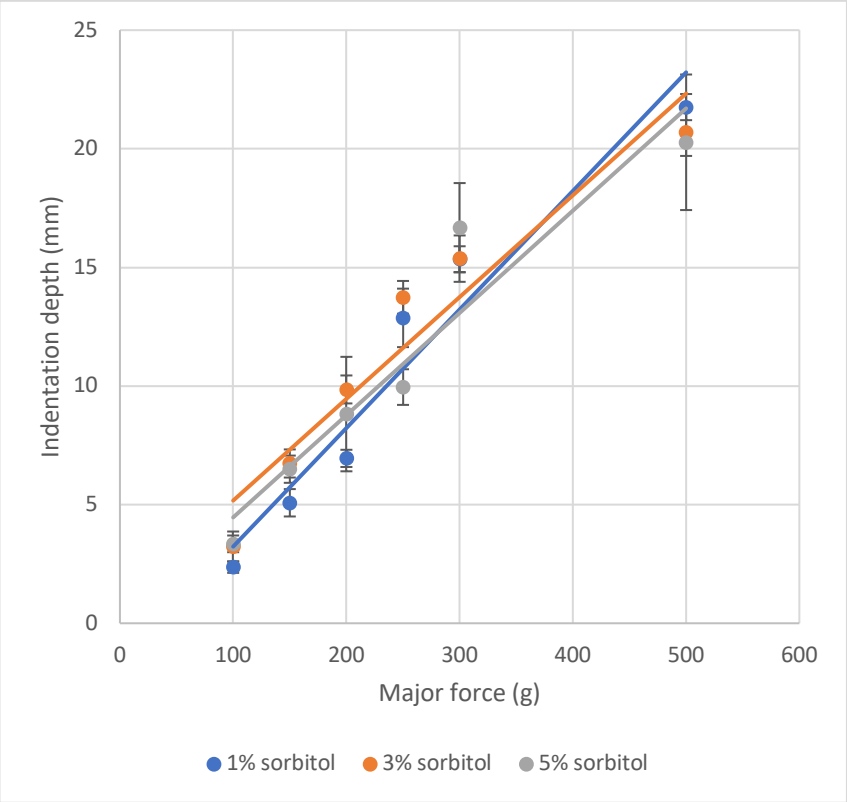

(b)

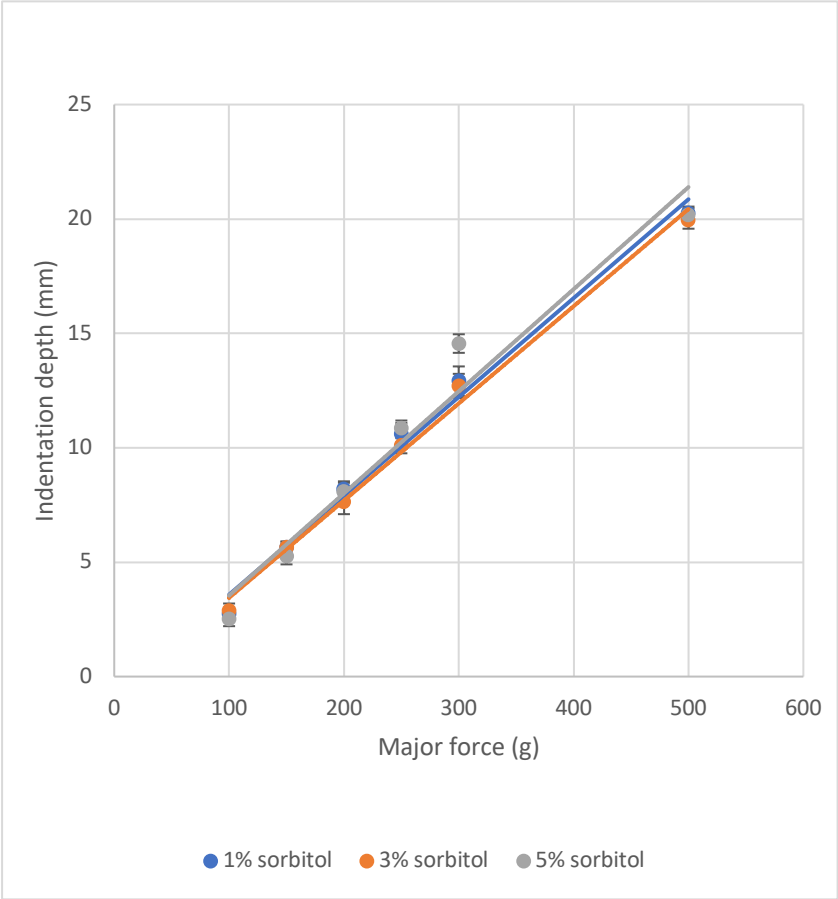

Figure 3-3 The effect of major force (g) on the (a)15% 220 bloom gelatin+ sorbitol foam and (b 15% 300 bloom gelatin+ sorbitol foam cubes.

(a)

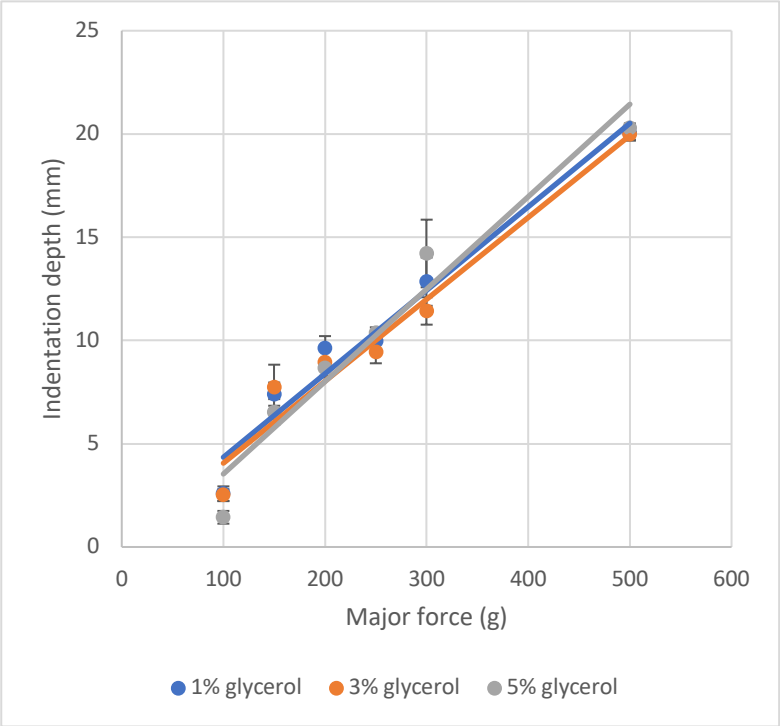

(b)

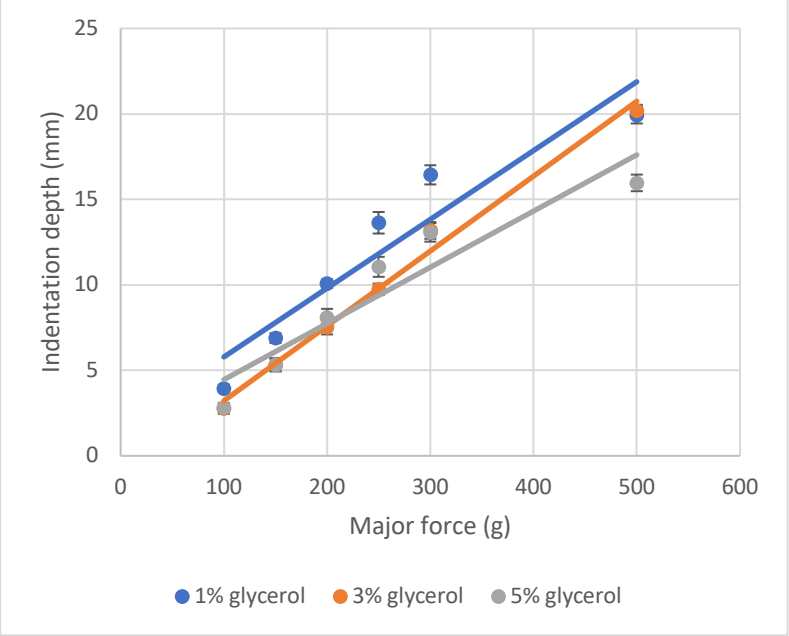

Figure 3-4 The effect of major force (g) on the (a)15% 220 bloom gelatin+ glycerol foam and (b)15%300 bloom gelatin+glycerol foam cubes.

(a)

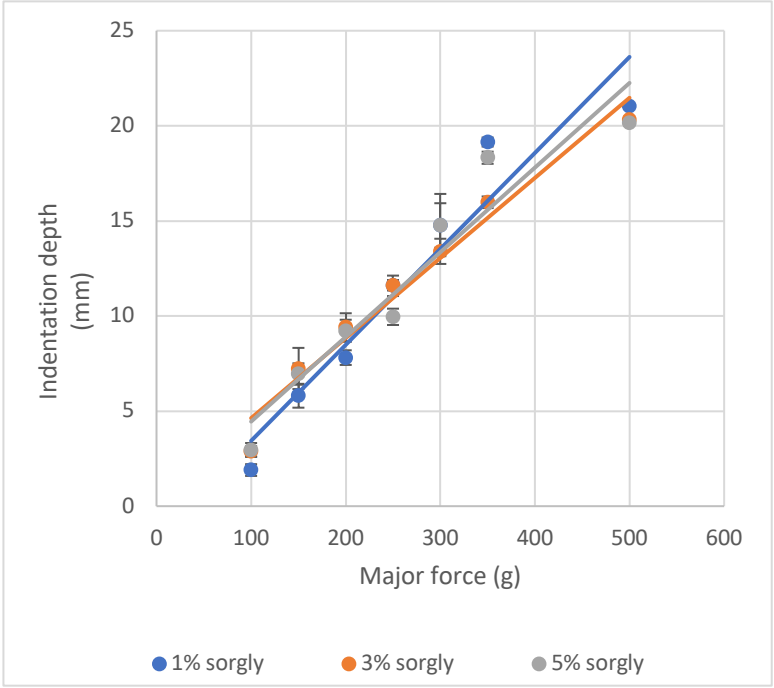

(b)

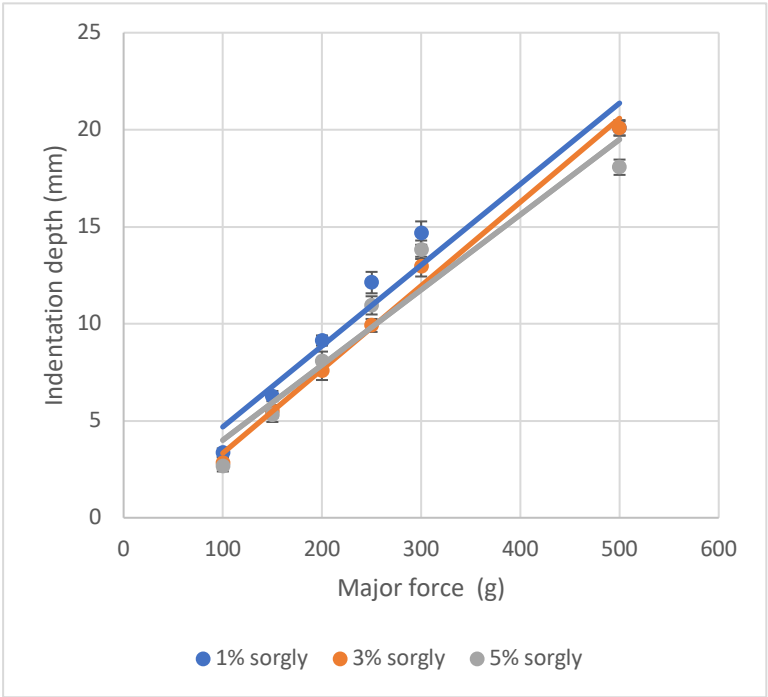

Figure 3-5 The effect of major force (g) on the (a)15% 220 bloom gelatin+ sorbitol and glycerol mixture foam and (b)15%300 bloom gelatin+ sorbitol and glycerol mixture foam cubes. Sorgly= sorbitol+glycerol.

In addition, it was noted that the 10% 220 and 300 bloom gelatins have given a less linear relationship, thus could be due to the material being too soft or that the indentation rod was applied on the surface of the phantoms it was placed on the edges and did not avoid it, thus an error in the measurements may have occur.

So, to apply the Young modulus on the experiment above we need to calculate the stress and strain, were stress is

$$Stress = \frac{F}{A}$$

where F is the force in N, A is the cross-sectional area in m^2 and stress is in N/m^2 or pascals (Pa). also, strain is known by

$$Strain = \frac{\Delta L}{L}$$

where ΔL is the extension of the original length in m and L is the original length in m, therefore the stress is unitless as it is the ratio of length measurements.

Therefore, the Young modulus (Y) is known as

$$Y = \frac{Stress}{Strain} = \frac{F * L}{A * \Delta L}$$

Young's modulus has a unit as for the stress N/m^2 or Pa, the change in the modulus is linear as the relation between the stress and strain is proportional but if the strain is increasing then these materials either go

under permanent deformation or break. Thus, in Figure 3-6 it can be seen the stress and strain curve of both the 220 and 300 bloom gelatin with the mixture of different concentration of sorbitol and glycerol. Hence, these different concentrations had the same linear relation, but it was the 3% mixture with the highest R^2 value which indicates that it is behaving more as an elastic material.

(a)

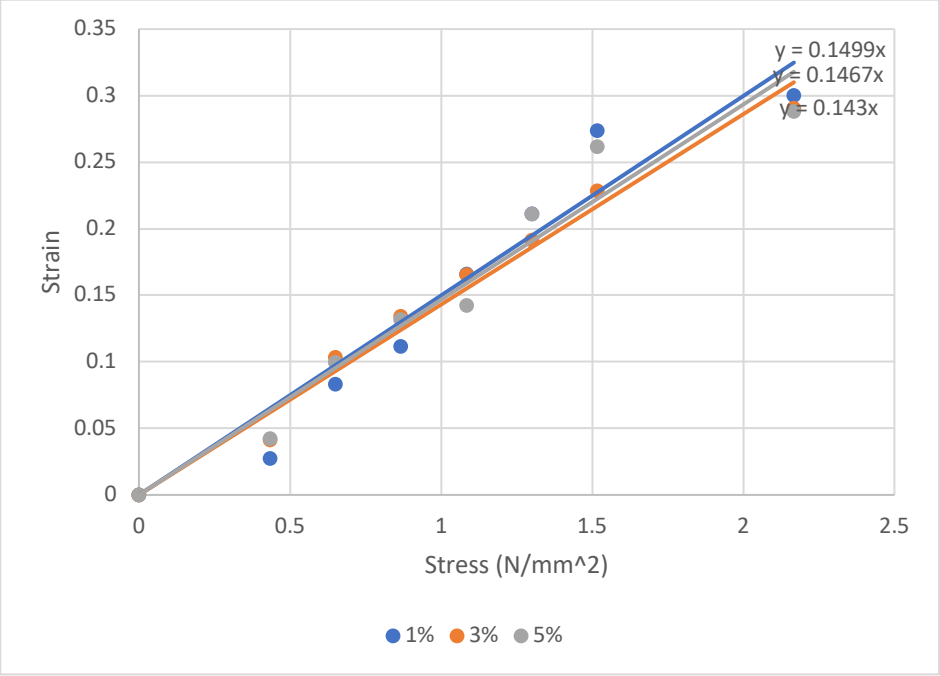

(b)

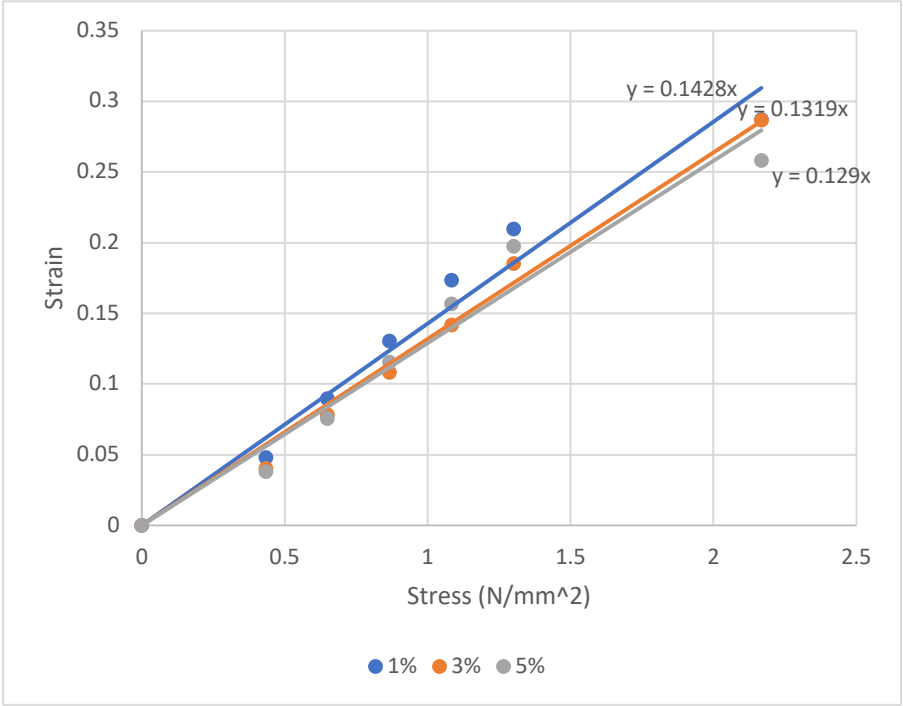

Figure 3-6 The stress and strain curve for (a) 15% 220 bloom+ sorbitol and glycerol mixture and (b) 15% 300 bloom + sorbitol and glycerol.

From, Figure 3-6 (a) the slope of the stress and strain curve of the 220 bloom foamed gelatin are 0.1499, 0.1467 and 0.143 mm^2/N for 1%, 3% and 5%, respectively. As for the slope of the stress and strain curve of the 300 bloom foamed gelatin are 0.1428, 0.1319 and 0.129 mm^2/N for 1%, 3% and 5%, respectively.

As for the stress and strain curve of the 220 bloom cubes it is shown in Figure 3-7 (a). It was calculated that the stress and strain slope is 0.0853, 0.076, and 0.0558 mm^2/N for 10%, 15% and 20%, respectively. The slope for the 300 bloom gelatin cubes is shown in

Figure 3-7 (b), the slope was calculated to be 0.0647, 0.053 and 0.0452 mm^2/N for 10%,15% and 20%, respectively.

(a)

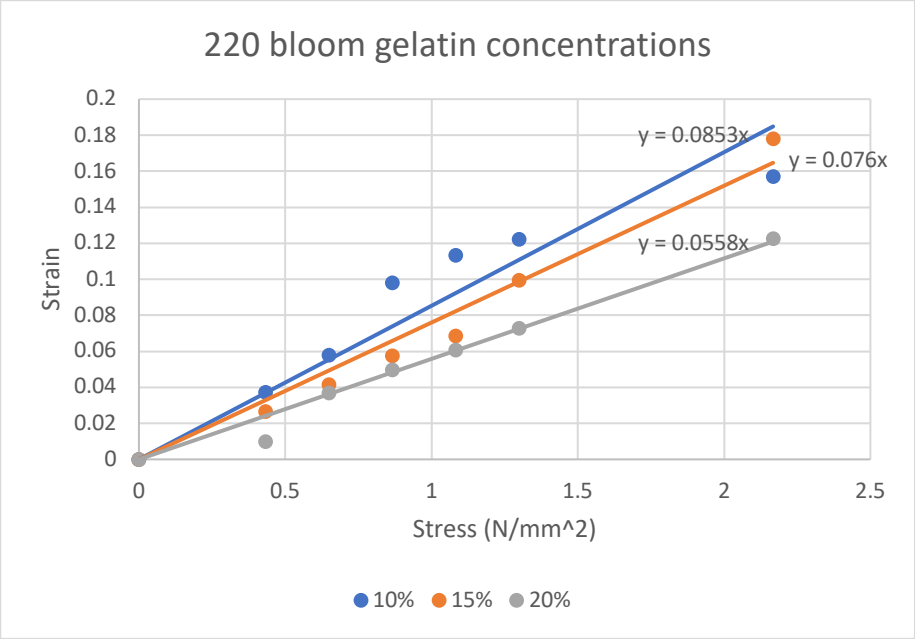

(b)

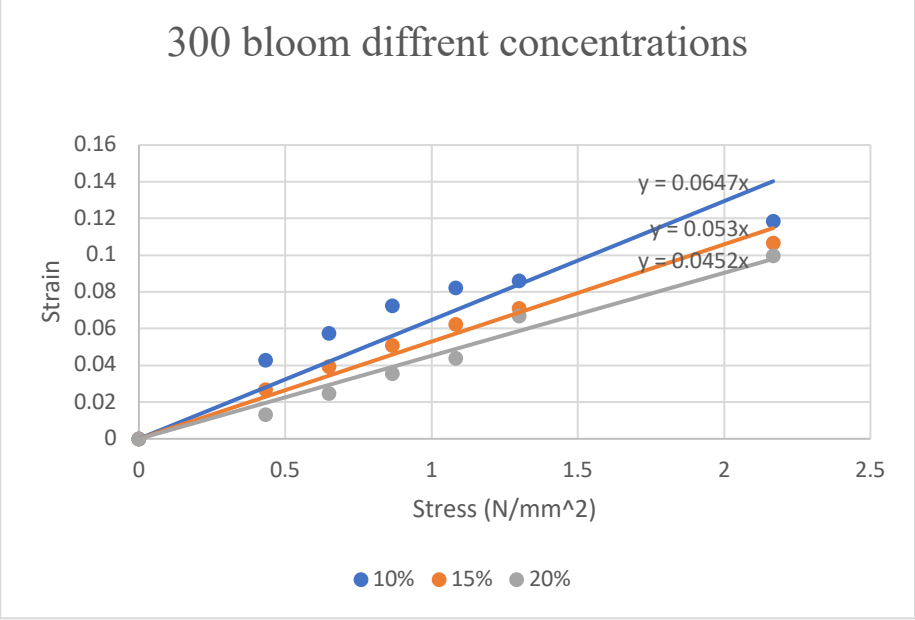

Figure 3-7 The stress and strain curve of (a) 200 bloom gelatin with different concentrations and (b) 300 bloom gelatin of different concentrations.

When comparing these slopes it was noted that with higher bloom concentration the slope was decreasing, it was also noted for high concentrations of sorbitol and glycerol the slope decreased too.

As for the radiological properties of the gelatin foam cubes, the cubes were imaged using a computed tomography scanner to obtain the densities of these foams. The CT scans were imported into Pinnacle for analysis. The density of the foamed cubes were 0.33 ± 0.16 and 0.33 ± 0.052 g/cm^3 for the mixtures that were frothed for 180 and 300 seconds, respectively. These densities are consistent as the human lung density. As for the mixtures that were whisked for 30 and 90 seconds, the densities were measured to be 0.9 ± 0.23 and 0.51 ± 0.45 g/cm^3, respectively. In addition, from Halberstadt *et al.* [51], they achieved a low-density foam equal or under 0.32 g /cm^3 by using santoprene material and foaming it using a foaming agent. We were able to achieve the same density by foaming the gelatin for 3 and 5 minutes.

4. Dose Response

The thin gelatin sheets (normal and foamed) were fabricated using the 300 bloom gelatin (10% by weight) and the stock solutions of Xylenol orange (XO) and Ferrous ammonium sulfate (Fe^{2+}). Hence, the preparation of 4 batches of 5 mm thin sheets. One of these thin sheets was not irradiated and was used as a reference. The thin sheets of gelatin FXO were irradiated using a 6 MV LINAC machine by 100, 200, 400, 600, 800, 1000 MU's. The thin sheets were sandwiched between 5.2 cm of polystyrene slabs, with the gelatin sheets located at the isocenter of the LINAC. After irradiation, the sheets changed their colour from yellowish-orange to dark orang and brown then purple due to the transformation of ferrous (Fe^{2+}) to ferric (Fe^{3+}).

Then, these sheets were evaluated using a spectrometer to calculate the absorbance. The spectrometer used is the HR4000, where the absorbance was measured at a specific wavelength (589 nm). From the measured data a positive correlation between the absorbance (unitless) and the irradiation dose (MU) as shown in Figure 4-1. The most sensitive batch is the 2 minutes foamed gelatin FXO sheets.

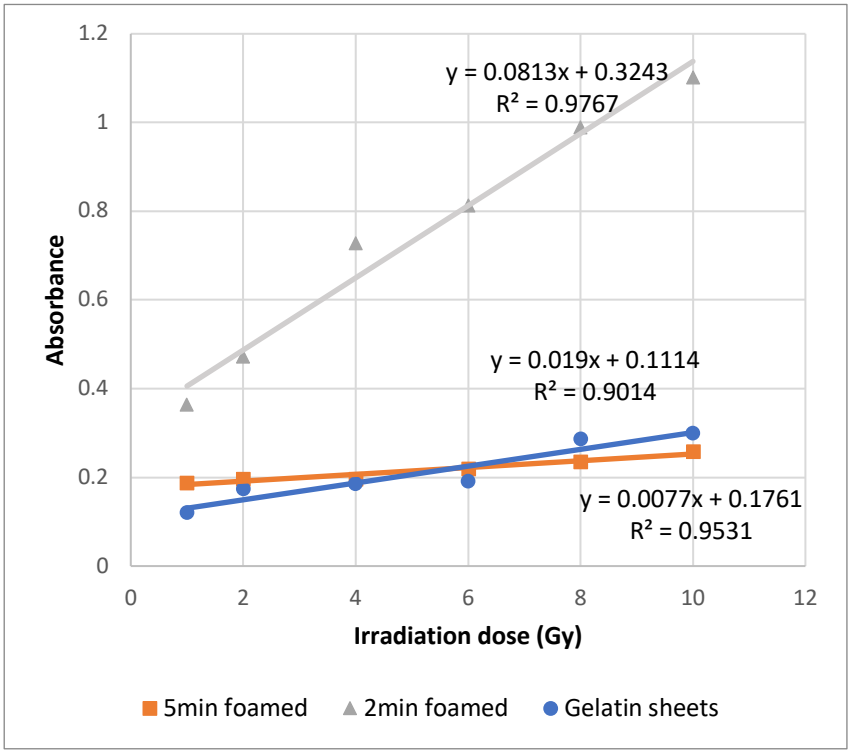

Figure 4-1 The effects of radiation on thin gelatin FXO sheets in blue, FXO gelatin sheets foamed for 2min in gray and FXO gelatin sheets for 5min in orange.

Then the sheets were analyzed using a spectrometer to calculate the absorbed dose and the attenuation coefficient in each sample. By using the Beer-Lambert law the absorbance (A) was calculated.

$$A = Log10\,(\frac{I_{\circ}}{I})$$

Then the linear attenuation coefficient (μ) was calculated using this equation were I_0 and I are the intensity going through and out of the sample, respectively. As for x it is the path length that the light crossed.

$$\mu = \frac{\ln {}^{I_\circ}/_{I}}{X}$$

Then the mass attenuation coefficient was calculated by dividing the linear attenuation coefficient (μ) by the density of the mixture (ρ), as shown in this equation:

$$Mass\ attenuation\ coefficient = \frac{\mu}{\rho}$$

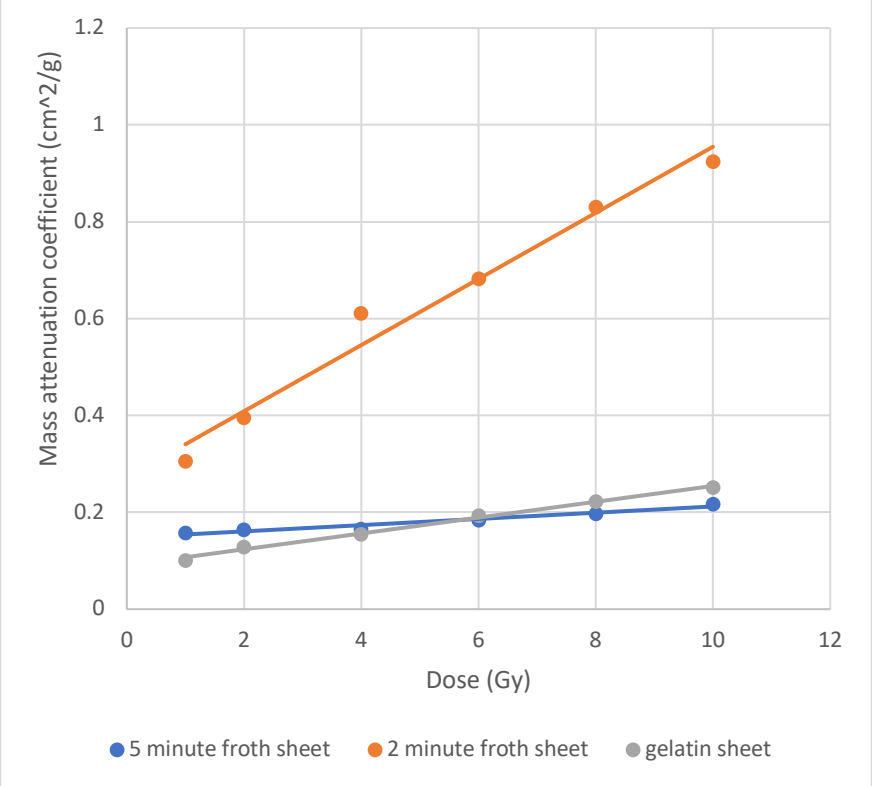

Figure 4-2 The relation between the irradiation dose and the mass attenuation coefficient.

From Figure 4-2 all the samples had a linear response, were the most sensitive response was in the 2 minutes foamed gelatin FXO. Hence, this sensitivity could be due to the scattering inside these sheets.

Jordan *et al.* [23], have measured FXO in gelatin previously at a specified wavelength (589 nm) to obtain the dose response curve, the linear attenuation coefficient was also found to be linear.

In addition, when the light travel through the thin gelatin and foamed sheets not all the light will transfer through these sheets, but some of the light will scatter and get absorbed. Therefore, we expected a higher overall attenuation. When fabricating these thin sheets a few air bubbles were there after these phantoms were cooled. When light passes through these bubbles some light scatters. Therefore, due to the scattered light the absorbance could also be overestimated.

5. Discussion

In the beginning of this research, three-dimensional cubes were fabricated using gelatin and foamed gels. The mechanical properties of these phantoms were measured. The elastic modulus of these gelatin and foams were obtained along with the Young modulus. From chapter 3, the concentration of these gels and foams had a negative relation with the indentation depth, so the higher the concentration of the mixture the less the indenter rode will travel through the phantom. Also, the gels phantoms which were fabricated using low concentration equal or less than 5% by weight, did not show any elastic properties as they were crushed under small major weights. The Hertz modulus adopts a complete elastic action in homogenises materials, but not all tissue mimicking materials will act as a completely elastic material. The stress and strain slope of the 220 bloom was calculated to be 0.0853, 0.076, and 0.0558 mm^2/N for 10%, 15% and 20%, respectively. The slope for the 300 bloom gelatin was calculated to be 0.0647, 0.053 and 0.0452 mm^2/N for 10%,15% and 20%, respectively.

The foamed gelatin phantoms were imaged using computed tomography to measure their densities. The foamed cubes had a density of 0.33 ± 0.16 and 0.33 ± 0.052 g/cm^3 for the mixture which was frothed for 180 and 300 seconds, respectively. This density is similar to the human lung density. The mixture that was whisked for 30 and 90 seconds the density was measured 0.9 ± 0.23 and 0.51 ± 0.45 g/cm^3,

respectively. Thus, it is shown that the longer the frothing time the smaller the error you would have in the measured density. That could be because the mixture is more homogeneous.

The second part of this research was to fabricate a thin sheet of radiochromic gels and foams and measure the absorbance using a simple optical spectroscopy instrument. The sheets of FXO gel and foam was irradiated using LINAC by 6 MV X-ray and the sheets were read out using the spectrometer 2 hours post irradiation. The measured absorbance was done at a specific wavelength (589 nm), the most sensitive sheet was the one frothed for 2 minutes as a highest response was observed. As for the 5 minutes foamed sheet it could be that due to the relatively long frothing time the mixture had so many air bubbles that leads the light to scatter inside the sheet.

The linear attenuation coefficient was measured for all the sheet samples and was noted that the change in it is linear. Also, in Figure 4-2 the mass attenuation was found to be linear for all the samples. That correlates to the paper published by Jorden *et al*. [23], that the linear attenuation coefficient in the dose response curve is linear.

The highest response was observed in the 2 minutes froth foamed gel, but that could be to the scattering inside the foamed sheets. Furthermore, the light, when passing through the sheet could scatter due to the air bubbles in the gel and foam sheets. This may lead to the overestimation or underestimation of the measured dose.

6. Conclusion

The aim of this research was to develop a gel dosimeter that has the same density as a human lung we achieved a density of 0.33 ± 0.16 g/cm^3 by frothing the gelatin mixture for three minutes while this density 0.33 ± 0.052 g/cm^3 was reached by frothing the gelatin mixture for five minutes. Also, we were able to measure the mechanical properties of the gels and foams, which may allow for developing a relationship between gelatins of different blooms and percentages of gelatin. The relationship between the stress and strain was found to be linear for all the concentration of the sorbitol and glycerol with 300-bloom gelatin. Specially, the 3% and 5% had an R^2 value of 1, which means that the ratio between the stress and strain was constant.

In addition, the FXO gels and FXO foams were irradiated with 6 MV photons and the optical properties were measured using a simple spectroscopy instrument. The absorbance was calculated using Beer-Lambert law and was found to be linear, especially for the 2 minutes foamed sheet. Also, the mass attenuation coefficient was measured and is linear for all the sheets mainly the 2 minutes foams was the most sensitive.

7. Future Work

The need of three-dimension dosimetry has developed rapidly in the last century, due to its ability to produce phantoms that replicate the human tissue and fabricate them in different and complex shapes. Gelatin is used as a gelling agent due to its easy fabrication and low cost. In this research, many experiments were done using gelatin to assess the mechanical properties of the gelatin, and the effect of radiation on the gelatin dosimeter (gel FXO). The need in the future is to be able to fabricate a human lung using gelatin and implanting a hard tumor inside of it. Based on the data arising from this preliminary study, it should be feasible to produce such phantoms.

8. References

[1] Prabhakar, R. (2013). Real-time dosimetry in external beam radiation therapy. World journal of radiology, 5(10), 352.

[2] Bernier, J., Hall, E. J., & Giaccia, A. (2004). Radiation oncology: a century of achievements. Nature Reviews Cancer, 4(9), 737.

[3] Porter, M. R. (Ed.). (1990). Recent developments in the technology of surfactants. Springer.

[4] Bushberg, J. T., & Boone, J. M. (2011). The essential physics of medical imaging. Lippincott Williams & Wilkins.

[5] Olding, T., L. Garcia, K. Alexander, L. J. Schreiner, and C. Joshi. "Stereotactic body radiation therapy delivery validation." In *Journal of Physics: Conference Series*, vol. 444, no. 1, p. 012073. IOP Publishing, 2013.

[6] Nasr, A. T., Alexander, K. M., Olding, T., Schreiner, L. J., & McAuley, K. B. (2015). Leuco-crystal-violet micelle gel dosimeters: II. Recipe optimization and testing. *Physics in Medicine & Biology*, *60*(12), 4685.

[7] Olding, T., Alexander, K. M., Jechel, C., Nasr, A. T., & Joshi, C. (2015). Delivery validation of VMAT stereotactic ablative body radiotherapy at commissioning. In *Journal of Physics: Conference Series* (Vol. 573, No. 1, p. 012019). IOP Publishing.

[8] Alexander, K. M., Pinter, C., Fichtinger, G., Olding, T., & Schreiner, L. J. (2018). Streamlined open-source gel dosimetry analysis in 3D slicer. *Biomedical Physics & Engineering Express*, *4*(4), 045041.

[9] DAY, M. J., & STEIN, G. (1950). CHEMICAL EFFECTS OF IONIZING RADIATION IN SOME GELS. NATURE, 166(4212), 146.

[10] ANDREWS, H. L., MURPHY, R. E., & LEBRUN, E. J. (1957). GEL DOSIMETER FORDEPTH-DOSE MEASUREMENTS. REVIEW OF SCIENTIFIC INSTRUMENTS, 28(5), 329-332.

[11] GORE, J. C., & KANG, Y. S. (1984). MEASUREMENT OF RADIATION DOSE DISTRIBUTIONS BY NUCLEAR MAGNETIC RESONANCE (NMR) IMAGING. PHYSICS IN MEDICINE & BIOLOGY, 29(10), 1189.

[12] ALEXANDER, P., CHARLESBY, A., & ROSS, M. (1954). THE DEGRADATION OF SOLID POLYMETHYLMETHACRYLATE BY IONIZING RADIATION. PROC. R. SOC. LOND. A,223(1154), 392-404.

[13] LAWTON, E. J., BUECHE, A. M., & BALWIT, J. S. (1953). IRRADIATION OF POLYMERS BY HIGH-ENERGY ELECTRONS. NATURE, 172(4367), 76.

[14] CHARLESBY, A., & ROSS, M. (1953). THE EFFECT OF CROSS-LINKING ON THE DENSITY AND MELTING OF POLYTHENE. PROC. R. SOC. LOND. A, 217(1128), 122-135.

[15] OLDHAM, M., SIEWERDSEN, J. H., SHETTY, A., & JAFFRAY, D. A. (2001). HIGH RESOLUTION GEL-DOSIMETRY BY OPTICAL-CT AND MR SCANNING. MEDICAL PHYSICS, 28(7), 1436-1445.

[16] POGUE, B. W., & PATTERSON, M. S. (2006). REVIEW OF TISSUE SIMULATING PHANTOMS FOR OPTICAL SPECTROSCOPY, IMAGING AND DOSIMETRY. JOURNAL OF BIOMEDICAL OPTICS, 11(4), 041102.

[17] ZANDI, M. (2008). STUDIES ON THE GELATION OF GELATIN SOLUTIONS AND ON THE USE OF RESULTING GELS FOR MEDICAL SCAFFOLDS (DOCTORAL DISSERTATION, UNIVERSITÄT DUISBURG-ESSEN, FAKULTÄT FÜR CHEMIE» PHYSIKALISCHE CHEMIE).

[18] THOMSON, R. C., WAKE, M. C., YASZEMSKI, M. J., & MIKOS, A. G. (1995).BIODEGRADABLE POLYMER SCAFFOLDS TO REGENERATE ORGANS. IN BIOPOLYMERS II (PP.245-274). SPRINGER, BERLIN, HEIDELBERG.

[19] SOLCHAGA, L. A., YOO, J. U., LUNDBERG, M., DENNIS, J. E., HUIBREGTSE, B. A., GOLDBERG, V. M., & CAPLAN, A. I. (2000). HYALURONAN-BASED POLYMERS IN THE TREATMENT OF OSTEOCHONDRAL DEFECTS. JOURNAL OF ORTHOPAEDIC RESEARCH, 18(5),773-780.

[20] NAM, Y. S., & PARK, T. G. (1999). BIODEGRADABLE POLYMERIC MICROCELLULAR FOAMS BY MODIFIED THERMALLY INDUCED PHASE SEPARATION METHOD. BIOMATERIALS, 20(19), 1783-1790.

[21] Nam, Y. S., & Park, T. G. (1999). Porous biodegradable polymeric scaffolds prepared by thermally induced phase separation. Journal of Biomedical Materials Research: An Official Journal of The Society for Biomaterials, The Japanese Society for Biomaterials, and The Australian Society for Biomaterials and the Korean Society for Biomaterials, 47(1), 8-17.

[22] Gelatin Gelatine collagen hydrolyzed collagen Gelatin manufactures, GMIA- Gelatin Manufacturers Institute of America Gelatin Handbook. (n.d.). Retrieved from http://www.gelatin-gmia.com/gelatinhandbook.html.

[23] Jordan, K., & Battista, J. (2004). Dose response of ferrous-xylenol orange gels: the effects of gel substrate, gelation time and dose fractionation. In Journal of Physics: Conference Series (Vol. 3, No. 1, p. 232). IOP Publishing.

[24] D'souza, W. D., Madsen, E. L., Unal, O., Vigen, K. K., Frank, G. R., & Thomadsen, B. R. (2001). Tissue mimicking materials for a multi-imaging modality prostate phantom. Medical physics, 28(4), 688-700.

[25] Low, D. (2015). The importance of 3D dosimetry. Journal of Physics: Conference Series, 573(1), 012009.

[26] Borgesa, J. A., Bencomo, J. A., Ibbott, G. S., & Ma, J. A Gel Lung-Equivalent Material for 3D Dosimetry.

[27] GUO, P. Y., ADAMOVICS, J. A., & OLDHAM, M. (2006). CHARACTERIZATION OF A NEW RADIOCHROMIC THREE-DIMENSIONAL DOSIMETER. MEDICAL PHYSICS, 33(5), 1338-1345.

[28] BALDOCK, C. (2009). HISTORICAL OVERVIEW OF THE DEVELOPMENT OF GEL DOSIMETRY: ANOTHER PERSONAL PERSPECTIVE. IN JOURNAL OF PHYSICS: CONFERENCE SERIES (VOL. 164, NO. 1, P. 012002). IOP PUBLISHING.

[29] KACZMAREK, K., HORNOWSKI, T., BIELAS, R., ŻAK, D., TIMKO, M., & JÓZEFCZAK, A. (2018). DEPENDENCE OF ULTRASONIC AND MAGNETIC HYPERTHERMIA ON THE CONCENTRATION OF MAGNETIC NANOPARTICLES. ACTA PHYSICA POLONICA A, 133(3), 716-718.

[30] Vieira, S. L., Pavan, T. Z., Junior, J. E., & Carneiro, A. A. (2013). Paraffin-gel tissue-mimicking material for ultrasound-guided needle biopsy phantom. *Ultrasound in medicine & biology*, *39*(12), 2477-2484.

[31] Lambert, S. M., Overturf III, G. E., Wilemski, G., Letts, S. A., Schroen-Carey, D., & Cook, R. C. (1997). Fabrication of low-density foam shells from resorcinol-formaldehyde aerogel. Journal of applied polymer science, 65(11), 2111-2122.

[32] Kim, H. W., Knowles, J. C., & Kim, H. E. (2004). Hydroxyapatite and gelatin composite foams processed via novel freeze-drying and crosslinking for use as temporary hard tissue scaffolds.

[33] Kailas, S. V. (n.d.). Chapter 17. Optical properties. Retrieved from https://nptel.ac.in/courses/112108150/pdf/Web_Pages/WEBP_M17.pdf

[34] Appleby, A., Christman, E. A., & Leghrouz, A. (1987). Imaging of spatial radiation dose distribution in agarose gels using magnetic resonance. *Medical physics*, *14*(3), 382-384.

[35] Baldock, C., Harris, P. J., Piercy, A. R., & Healy, B. (2001). Experimental determination of the diffusion coefficient in two-dimensions in ferrous sulphate gels using the finite element method. Australasian Physics & Engineering Sciences in Medicine, 24(1), 19.

[36] Maryanski, M. J., Gore, J. C., & Schulz, R. J. (1992). 3-D radiation dosimetry by MRI: solvent proton relaxation enhancement by radiation-controlled polymerisation and cross-linking in gels. Proc. Int. Soc. for Magnetic Resonance in Medicine (New York).

[37] Baldock, C., De Deene, Y., Doran, S., Ibbott, G., Jirasek, A., Lepage, M., ... & Schreiner, L. J. (2010). Polymer gel dosimetry. Physics in Medicine & Biology, 55(5), R1.

[38] Baldock, C., Burford, R. P., Billingham, N., Wagner, G. S., Patval, S., Badawi, R. D., & Keevil, S. F. (1998). Experimental procedure for the manufacture and calibration of polyacrylamide gel (PAG) for magnetic resonance imaging (MRI) radiation dosimetry. Physics in Medicine & Biology, 43(3), 695.

[39] Baldock, C., & Watson, S. (1999). Risk assessment for the manufacture of radiation dosimetry polymer gels. In Proc. 1st Int. Workshop on Radiation Therapy Gel Dosimetry. Lexington, KY, USA (pp. 154-156).

[40] Niroomand-Rad, A., Blackwell, C. R., Coursey, B. M., Gall, K. P., Galvin, J. M., McLaughlin, W. L., ... & Soares, C. G. (1998). Radiochromic film dosimetry: recommendations of AAPM radiation therapy committee task group 55. Medical physics, 25(11), 2093-2115.

[41] Ataei, P. (2012). Development of a transparent and deformable two dimensional radiochromic gel dosimeter(Doctoral dissertation).

[42] Armstrong, W. A., & Grant, G. A. (1958). Radiation chemistry of solutions: I. Use of leuco triarylmethane compounds for chemical dosimetry. Radiation research, 8(5), 375-387.

[43] Gupta, B. L., & Narayan, G. R. (1985). G (Fe3+) values in the FBX dosemeter. Physics in Medicine & Biology, 30(4), 337.

[44] Gupta, B. L., & Madhvanath, U. (1985). G (Fe3+) values in the FBX dosimeter at low dose-rates. The International Journal of Applied Radiation and Isotopes, 36(12), 985-987.

[45] Chahat, N., Zhadobov, M., & Sauleau, R. (2012). Broadband tissue-equivalent phantom for BAN applications at millimeter waves. IEEE Transactions on Microwave Theory and Techniques, 60(7), 2259-2266.

[46] Onishi, T., & Uebayashi, S. (2006). Biological tissue-equivalent phantoms usable in broadband frequency range. NTT DoCoMo Tech. J, 7, 61-65.

[47] Ølberg, S., Skretting, A., Bruland, Ø., & Olsen, D. R. (2000). Dose distribution measurements by MRI of a phantom containing lung tissue equivalent compartments made of ferrous sulphate gel. Physics in Medicine & Biology, 45(10), 2761.

[48] De Deene, Y., Claeys, C., & De Wagter, C. (2006). Three dimensional radiation dosimetry in lung-equivalent regions by use of a radiation sensitive gel foam: Principles. In Journal of Physics: Conference Series (Vol. 56, No. 1, p. 256). IOP Publishing.

[49] Adams, H., Bernard, M. S., & McConnochie, K. (1991). An appraisal of CT pulmonary density mapping in normal subjects. Clinical radiology, 43(4), 238-242.

[50] Salerno, A., Oliviero, M., Di Maio, E., & Iannace, S. (2007). Thermoplastic foams from zein and gelatin. International Polymer Processing, 22(5), 480-488.

[51] Halberstadt, L., Mertinooke, P. E., Perry, J. V., & Muessel, D. C. (1995). Method and Apparatus for Extruding a Low Density Thermoplastic Foam.

[52] Long, R., Hall, M. S., Wu, M., & Hui, C. Y. (2011). Effects of gel thickness on microscopic indentation measurements of gel modulus. Biophysical journal, 101(3), 643-650.

[53] Czerner, M., Fellay, L. S., Suárez, M. P., Frontini, P. M., & Fasce, L. A. (2015). Determination of elastic modulus of gelatin gels by indentation experiments. Procedia Materials Science, 8, 287-296.

[54] Lin, D. C., Dimitriadis, E. K., & Horkay, F. (2007). Elasticity Models for the Spherical Indentation of Gels and Soft Biological Tissues. MRS Online Proceedings Library Archive, 1060.

[55] Ternovskii, A. P., Alekhin, V. P., Shorshorov, M. K., Khrushchev, M. M., & Skvortsov, V. N. (1973). The character of the variation of microhardness with indentation size and the deformation behavior of materials under conditions of concentrated surface loading. Zavodskaya Laboratoriya, 39, 1242.

[56] Bulychev, S. I., Alekhin, V. P., Shorshorov, M. K., & Ternovskii, A. P. (1976). Mechanical properties of materials studied from kinetic diagrams of load versus depth of impression during microimpression. Strength of Materials, 8(9), 1084-1089.

[57] Doerner, M. F., & Nix, W. D. (1986). A method for interpreting the data from depth-sensing indentation instruments. Journal of Materials research, 1(4), 601-609.

[58] Oliver, W. C., & Pharr, G. M. (1992). An improved technique for determining hardness and elastic modulus using load and displacement sensing indentation experiments. Journal of materials research, 7(6), 1564-1583.

[59] Loubet, J. L., Georges, J. M., Marchesini, O., & Meille, G. (1984). Vickers indentation curves of magnesium oxide (MgO). Journal of tribology, 106(1), 43-48.

[60] Gregorič, G. Elasticity of biological gels.

[61] Okamura, A. M., Simone, C., & O'leary, M. D. (2004). Force modeling for needle insertion into soft tissue. IEEE transactions on biomedical engineering, 51(10), 1707-1716.

[62] Roesthuis, R. J., Van Veen, Y. R., Jahya, A., & Misra, S. (2011, September). Mechanics of needle-tissue interaction. In Intelligent Robots and Systems (IROS), 2011 IEEE/RSJ International Conference on (pp. 2557-2563). IEEE.

[63] Duriez, C., Guébert, C., Marchal, M., Cotin, S., & Grisoni, L. (2009, September). Interactive simulation of flexible needle insertions based on constraint models. In International Conference on Medical Image Computing and Computer-Assisted Intervention (pp. 291-299). Springer, Berlin, Heidelberg.

[64] Smith, S. T., Masters, K. S., Hosokawa, K., Blinco, J., Crowe, S. B., Kairn, T., & Trapp, J. V. (2015). A reduction of diffusion in PVA Fricke hydrogels. In Journal of Physics: Conference Series (Vol. 573, No. 1, p. 012046). IOP Publishing.

[65] Oglat, A. A., Matjafri, M. Z., Suardi, N., Oqlat, M. A., Abdelrahman, M. A., Oqlat, A. A., ... & Abujazar, M. Y. (2018). Chemical items used for preparing tissue-mimicking material of wall-less flow phantom for doppler ultrasound imaging. Journal of medical ultrasound, 26(3), 123.

[66] Liosi, G. M., Dondi, D., Vander Griend, D. A., Lazzaroni, S., D'Agostino, G., & Mariani, M. (2017). Fricke-gel dosimeter: overview of Xylenol Orange chemical behavior. *Radiation Physics and Chemistry*, *140*, 74-77.

[67] Eyadeh, M. (2015). *The Development of a Transparent Poly (vinyl alcohol) Radiochromic Cryogel Dosimeter and Optical Detection Methods* (Doctoral dissertation).

[68] Adamovics, J., & Maryanski, M. J. (2003). New 3D radiochromic solid polymer dosimeter from leuco dyes and a transparent polymeric matrix. *Medical Physics*, *30*(6), 1349.

[69] Kan, S. H. (n.d.). Metrics and Models in Software Quality Engineering, Second Edition. Retrieved from https://learning.oreilly.com/library/view/metrics-and-models/0201729156/ch07.html

[70] Labeled Diagram of the Human Lungs. (n.d.). Retrieved from https://bodytomy.com/labeled-diagram-of-human-lungs